博士論文

固体 NMR の新規測定手法の開発
及び製剤固体物性の定性・定量分析への適用

2017 年 03 月

朝田　麻実子

博士論文

固体 NMR の新規測定手法の開発
及び製剤固体物性の定性・定量分析への適用

Development of New Techniques for Solid State NMR and Application to Qualitative and Quantitative Analysis on the Solid State Properties in Pharmaceuticals

本論文は静岡県立大学大学院薬学研究院
博士論文である

2017 年 03 月
March, 2017

朝田　麻実子
Mamiko Asada

CONTENTS

LEXICON

^{13}C: Carbon-13

^{19}F: Fluorine-19

^{19}F T_1: Fluorine-19 spin-lattice relaxation time

^{19}F T_{1rho}: Fluorine-19 spin-lattice relaxation time in the rotating frame

^{1}H: Proton

^{1}H T_1: Proton spin-lattice relaxation time

^{1}H T_{1rho}: Proton spin-lattice relaxation time in the rotating frame

Continuous wave (CW) decoupling: A technique to remove heteronuclear dipolar coupling by applying continuous irradiation at the frequency of the proton resonance.

Cross-polarization (CP): Transfer of magnetization from an abundant spin (e.g. ^{1}H) to another spin (normally a dilute spin; e.g. ^{13}C or ^{15}N) to utilize proton magnetization which has a short relaxation time in order to reduce experimental duration and/or to obtain sufficient signal-to-noise ratio.

Cross-polarization with the magic angle spinning (CP-MAS): The most common technique in solid state NMR. The combination of cross-polarization, magic angle spinning and dipolar decoupling eliminates the dipolar interaction between an abundant spin (e.g. ^{1}H) and another spin (normally a dilute spin; e.g. ^{13}C or ^{15}N), to provide high resolution and sensitivity of the spectrum.

Dipolar decoupling (DD): A technique to eliminate the heteronuclear dipolar interaction between an abundant spin (e.g. ^{1}H) and another spin (normally a dilute spin; e.g. ^{13}C or ^{15}N) by irradiating the strong high-frequency electromagnetic wave to an abundant spin (e.g. ^{1}H).

Dipolar decoupling-magic angle spinning with single pulse (DD-MAS): A technique of direct excitation for an observed spin (normally a dilute spin; e.g. ^{13}C or ^{15}N) with dipolar decoupling (DD), which eliminates the heteronuclear dipolar interaction between an abundant spin (e.g. ^{1}H) and another spin (normally a dilute spin; e.g. ^{13}C or ^{15}N), combined with magic angle spinning (MAS, v.i.).

Flip-back (FB) pulse: A technique to force proton magnetization on the transverse axis to the longitudinal axis after acquisition of the observed nuclei in order to reduce relaxation delay time between scans.

Inversion-recovery pulse sequence: A pulse sequence which uses a 180 degree RF pulse that inverts the magnetization followed by a 90 degree RF pulse (v.i.) that brings the residual longitudinal magnetization into the x-y or transverse plane. The method causes the transition of signals from negative to positive, with passage through the null point.

Magic angle spinning (MAS): The sample is mechanically flipped against the external magnetic field at the magic angle (θ = 54.74°) and rotated at high-speed to eliminate or average out the chemical shift anisotropy.

Nuclear magnetic resonance (NMR): Phenomenon of interaction between an atomic nucleus in a static magnetic field and the unique frequency of an electromagnetic wave.

Proton (^{1}H) decoupling: A technique to eliminate the heteronuclear dipolar interaction between an abundant spin (e.g. ^{1}H) and another spin (normally a dilute spin; e.g. ^{13}C or ^{15}N) by irradiating a strong high-frequency electromagnetic wave to an abundant spin (e.g. ^{1}H).

Proton spin-lattice relaxation time (^{1}H T_1): Longitudinal relaxation time. The process of the return of the magnetization vector to the ground state by energy release, which causes a return to the longitudinal axis.

Proton spin-lattice relaxation time in the rotating frame (^{1}H T_{1rho}): Longitudinal relaxation time of the rotating frame.

Relaxation delay time (RD): Recovery time for the return of the whole magnetization to the ground state. It is set in the beginning of the pulse sequence.

Relaxation filter-selective signal excitation (RFS) methods: Selective signal excitation methods newly developed by the author.

RF pulse: Radio frequency wave pulse. Electromagnetic frequency wave which vertically irradiates toward a static magnetic field.

Small-tip-angle RF pulse: RF pulse to flip the nuclear spin to less than 90° from the ground state.

Spin-locking: Irradiation of the radio frequency wave pulse from the y transverse plane to prevent phase shifting and to lock the nuclear spin magnetization to observe the decay of magnetization.

SPINAL-64: A multi-pulse decoupling sequence of an extension of TPPM (v.i.) which disperses the ^{1}H magnetization all over the transverse plane. Decoupling efficiency is higher than CW decoupling.

SP-MAS (single pulse-magic angle spinning): The technique of direct excitation of an observed spin (normally a dilute spin; e.g. ^{13}C or ^{15}N) without dipolar decoupling.

Tau (τ) delay: Interval of time for the return of magnetization to the ground state for RFS methods. It is set before the acquisition step in the pulse sequence which will be optimized for the selective signal excitation for each of the objective compounds.

Two-pulse phase modulation (TPPM): A multi-pulse decoupling sequence which disperses the ^{1}H magnetization all over the transverse plane. Decoupling efficiency is higher than CW decoupling.

ABBREVIATIONS

API: Active pharmaceutical ingredients

Acq: Acquisition

ATC: Atorvastatin calcium

β-CD: β-Cyclodextrin

CP: Cross-polarization

CP-MAS: CP with magic angle spinning

CW: Continuous wave

DD: Dipolar decoupling

DD-MAS: Dipolar decoupling-magic angle spinning with single pulse

DECRA: Direct exponential curve resolution algorithm

DOSY: Diffusion ordered spectroscopy

DSC: Differential scanning calorimetry

FB: Flip-back

^{1}H Dec.: Proton decoupling

MAS: Magic angle spinning

NMR: Nuclear magnetic resonance

PLS: Partial least squares

PVP: Polyvinylpyrrolidone

RD: Relaxation delay time

RFS: Relaxation filter-selective signal excitation

RF pulse: Radio frequency pulse

ROSY: Relaxation ordered spectroscopy

SPINAL-64: Small phase incremental alternation with 64 steps

SP-MAS: Single pulse-magic angle spinning

TMS: Tetramethylsilane

TOSY: Rate of relaxation ordered spectroscopy

TPPM: Two-pulse phase modulation

XRPD: X-ray powder diffraction

INTRODUCTION

Many solid pharmaceuticals consist of a number of components as drug substances and excipients. Understanding the solid state properties of pharmaceuticals is important because changes in them may affect solubility, bioavailability, processability, and physical/chemical stability.[1] The development of practical analytical methods for pharmaceuticals which allow the independent evaluation of each component without physical isolation would therefore be useful. Also, pharmaceuticals are typically manufactured in a stable crystalline form, because the amorphous form tends to convert to the crystalline form due to its thermodynamic instability. At the same time, however, the amorphous forms of active pharmaceutical ingredients (APIs) have attracted considerable interest due to their enhanced dissolution rate compared with poorly soluble crystalline forms, which may improve the therapeutic efficacy of these drugs. Whichever solid state form is chosen, it is important to ensure that this form is not contaminated by other solid state forms, from the viewpoints of stability and patenting issues, among others.[2]

Quantitative analysis methods traditionally used for trace amounts of crystalline contents include X-ray powder diffraction (XRPD), thermal analysis such as differential scanning calorimetry (DSC) or microcalorimetry, and vibration spectroscopy (Raman, infrared or near-infrared spectroscopy) combined with multivariate analysis.[3, 4] These methods have low sensitivity, however, which might prevent their use in detecting trace amounts of crystalline contents in pharmaceutical formulations.

The marked importance of nuclear magnetic resonance (NMR) spectroscopy as an analytical technique in pharmaceutical sciences has recently been recognized. In particular, solid state NMR has many characteristics which are not shared by the alternative analytical methods, such as non-destructive analysis, high resolution, high specificity, quantitative analysis and the provision of structural information.

NMR has a unique phenomenon called relaxation, the process in which nuclear spin returns to the original ground state by releasing previously absorbed energy. Nuclear spins trend in various directions without an external magnetic field. Nuclear spins split into the magnetic field direction in parallel with the external magnetic field and in the inverse direction in accordance with a thermal Boltzmann distribution in the presence of an external magnetic field. The energy of nuclear spins of the inverse magnetic field direction is slightly higher because they go against the external magnetic field and thus the number is low. Excessive nuclear spins transfer from a lower energy level to a higher energy level by providing the energy corresponding to this energy difference in the form of radio waves to resonate the nuclear magnet. Phase shifting gradually occurs when the radio waves which induce excited-state nuclide are stopped, and nuclear spins return to the original ground state by releasing energy. This process when nuclear spins return from the excited state to the ground state is called relaxation. The first relaxation process which occurs with phase shifting is called T_2, or “transverse” or “spin-spin” relaxation time, and the next process in the return to the original ground state by the release of energy is called T_1, or “longitudinal” or “spin-lattice” relaxation time.

In addition to these two types of relaxation time, there is longitudinal relaxation time in the rotating frame called $T_{1rho,}$ which is the process in which the magnetization vector decays under spin-locking of the nuclear spin.

In contrast to solution NMR, extreme line broadening of signal occurs in solid state NMR by dipolar interaction between two nuclear magnets of abundant spin (e.g. ^{1}H) and a dilute spin (e.g. ^{13}C or ^{15}N), and chemical shift anisotropy, which originates from random molecular orientation against the external magnetic field. There are two successful methods to removing these influences and sharpening the signals. One is dipolar decoupling (DD), which eliminates heteronuclear dipolar interaction by irradiating the strong high-frequency electromagnetic ray to ^{1}H nuclei. The second is magic angle spinning (MAS), which mechanically flips the sample against the external magnetic field at the magic angle and rotates the sample at a high speed. Further, they are combined with cross polarization (CP), which transfers the magnetization from an abundant spin (e.g. ^{1}H) to a dilute spin (e.g. ^{13}C or ^{15}N) to utilize proton magnetization, which has a short relaxation time to reduce experimental duration or obtain sufficient signal-to-noise ratio (called CP-MAS). This is the most popular method used in solid state NMR. There is no quantitative performance between the respective signal areas and the number of carbons because CP-MAS uses the magnetization transfer based on the dipolar interaction between an abundant spin and a dilute spin during cross polarization, whose efficiency depends on molecular motion and internuclear distances.

While a number of useful pulse sequences have been developed for pure substances, these require sample isolation and purification before data collection. Attempts at analysis without such isolation and purification are often confounded by signal overlap between components in a mixture spectrum, with subsequent complication of results.

To facilitate the acquisition of NMR spectra of individual components in a mixture of two or more compounds, several techniques without physical isolation have been

developed. For solution NMR, the spectra of individual components can be separated using diffusion ordered spectroscopy (DOSY),[5-7] a technique based on the difference in self-diffusion coefficients, which are unique to each component. For solid state NMR, previous methods separate the spectra of individual components by mathematical analytical processing methods, such as the direct exponential curve resolution algorithm (DECRA), which requires equally spaced data sampling in proton spin-lattice relaxation time (^{1}H T_1),[8, 9] and 2-dimensional experiments, such as the rate of relaxation ordered spectroscopy (TOSY)[10] and relaxation ordered spectroscopy (ROSY)[11] using ^{1}H T_1 or proton spin-lattice relaxation time in the rotating frame (^{1}H T_{1rho}). However, these methods are time-consuming (approximately 10–50 h), restricted in their scope of data collection, and require complicated data analysis or have low accuracy, which limit their practicality of use.

NMR spectroscopy is inherently quantitative because signal intensity is proportional to the number of distinct sites in the components. With regard to quantitative ^{13}C solid state NMR spectroscopy, however, several experimental aspects need to be taken into consideration. The spectra acquired with cross-polarization (CP), which is used to transfer the magnetization from an abundant spin (^{1}H) to a dilute spin (e.g. ^{13}C or ^{15}N), may distort the relative intensities because CP efficiency is not unique to individual components. Also, determining the total intensity of signal from a given site by integration may be difficult due to overlapping broad lines and the presence of other components, particularly excipients in formulated products. Common strategies for overcoming these problems with quantitation in solid state NMR are the application of signal deconvolution, signal subtraction, or partial least squares (PLS) analysis with several fitting parameters, as the signals from different

crystalline polymorphic forms or broad amorphous signals and crystalline signals often overlap.[4, 12-16]

This complexity thus points to the need for a simple and versatile method which allows direct observation and accurate quantitation of a target component in a formulated product by selective excitation of the target signals only. As remarkable features of solid state NMR compared to solution NMR, the differences in local intramolecular mobility (rotation, vibration etc.), whole molecular mobility, and/or intermolecular interaction appear as substantial differences in relaxation times (T_1, T_{1rho} and/or T_2) in solid state NMR. In addition to these characteristics, the author focused on two characteristics of solid state ^{13}C NMR. One is that the proton relaxation time is equalized in one component because rapid intra domain spin diffusion is caused by strong ^{1}H-^{1}H homonuclear dipolar couplings in solid samples. The other is that individual components have a unique proton relaxation time, which results from the molecular mobility of the material. From these characteristics, the difference in proton relaxation time can be used to selectively excite ^{13}C signals of individual components in formulated products.

The author firstly developed two new relaxation filter-selective signal excitation (RFS) methods in ^{13}C solid state NMR using ^{1}H spin-lattice relaxation time in the rotating frame (^{1}H T_{1rho}) to extract the spectrum of a target component from a formulated product. One involves selective ^{13}C signal excitation of the component with the longest ^{1}H T_{1rho}, and the other involves that for the other components, which have various types of ^{1}H T_{1rho} (termed the RFS method for long ^{1}H T_{1rho} and the RFS method for selective ^{1}H T_{1rho}. Further, the author was able to successfully apply spin-locking at low power in selective signal excitation, thereby reducing damage to NMR systems and increasing the usability of a long spin-lock time.

The author applied these methods to the selective ^{13}C signal excitation of each component in a commercially available drug containing several active pharmaceutical ingredients, and also to a mixture of two saccharides. In addition, the author also applied one of the developed RFS methods to the quantitative analysis of a mixture of crystals and amorphous solid dispersion of nifedipine with polyvinylpyrroridone (PVP) K-30, and to a polymorphic mixture of indomethacin α form and γ form. The author successfully obtained linearity for crystallinity or quantitation over a wide range of 5% to 100%.

One problem with these methods is that they are unsuitable when components have a similar ^{1}H T_{1rho}. However, such components might also differ in their ^{1}H spin-lattice relaxation time (^{1}H T_1), which would allow selective extraction of the spectrum of a target component in a mixture.

The author developed a new method which utilizes the difference in ^{1}H T_1 of each component and decay of proton magnetization to null to extract the spectrum of a target component with the longest ^{1}H T_1 in a mixture (termed the RFS method for long ^{1}H T_1). A second approach to selectively exciting the ^{13}C signals of those components with long or short ^{1}H T_1 uses an inversion-recovery pulse sequence (180°–τ–90°) on proton magnetization before the CP step.[17, 18] The author initially applied this method to pharmaceutical applications, and expanded its use to quantitative analysis with direct signal integration (termed the RFS method for selective ^{1}H T_1). These methods are simple as they are one-dimensional experiments and provide a considerable reduction in experimental duration compared to the existing methods,[4, 12-16] and provide direct and accurate qualitative and quantitative analysis of each component in a mixture.

Nevertheless, selective signal excitation of a target component from a multicomponent mixture using a single RFS method is sometimes difficult. The author therefore developed several new RFS methods which combine several types of RFS method to extract the target component from a multicomponent mixture in a single experiment. The author used these combined RFS methods to successfully selectively extract the target component from a commercially available drug which contained multiple active ingredients and excipients.

The author also developed these RFS methods by applying a flip-back (FB) pulse[12, 19-21] to shorten the experimental duration or to increase the relative signal intensity of the component. This was done by forcing the proton magnetization on the transverse axis to the longitudinal axis after acquisition of the ^{13}C signals in the CP with the magic angle spinning (CP-MAS) experiment.

Though the author has developed practical methods with ^{13}C solid state NMR, higher sensitivity is sometime necessary; for example, in the case that it is necessary to confirm the crystallinity of API in quite low-dose pharmaceuticals.

One method which does not suffer from low sensitivity is fluorine-19 MAS NMR spectroscopy. The high gyromagnetic ratio and 100% isotopic abundance of fluorine atoms (^{19}F) ensures high sensitivity within an extremely short experimental duration, even for diluted systems. Fluorine-19 solid state NMR spectroscopy has been applied not only to pharmaceutical science,[22-24] but also to polymer sciences with the development of useful pulse sequences.[25-27] Further, the fluorine atom is a relatively frequent component of pharmaceutical drugs[28] and is not overwrapped by signals of the components of general excipients. Owing to the problem of signal overlapping, however, conventional ^{19}F CP-MAS, DD-MAS (dipolar decoupling-magic angle spinning with single pulse) or SP-MAS (single pulse-magic angle spinning) cannot

always be used for the precise quantitative analysis of trace amounts of crystalline contents in mixtures of crystalline polymorphs, or in mixtures of crystalline and amorphous forms of the same chemical compounds.

Based on the RFS methods the author previously developed in ^{13}C solid state NMR, the author initially applied these RFS methods to ^{19}F solid state NMR. These methods can be applied to the quantitative analysis of contaminated or partially changed crystalline phase from amorphous API in tablets. For testing, the author selected atorvastatin calcium (ATC), which is known to exist in a variety of polymorphic forms (41 crystalline and 2 amorphous forms).[23, 24, 29, 30] The author applied these methods to detecting trace amounts of the crystalline phase in ATC tablets containing mainly the amorphous form of ATC, which were supplied by two generic drug suppliers.

RESULTS AND DISCUSSION

The author developed several new RFS methods in 13C solid state NMR and 19F solid state NMR for pharmaceutical applications. The author found that these methods were able to be used in both qualitative and quantitative analyses with accurate estimation, allowing for rapid assessment of formulated products, polymorphic mixtures, and mixtures of crystalline and amorphous phases. Characteristic features of these RFS methods over existing selective excitation and quantitative analysis methods included time efficiency, simplicity of conduct, supply of direct information, and utility in quantitative analysis.

CHAPTER 1

The RFS methods for ^{1}H T_{1rho} in ^{13}C solid state NMR spectroscopy

1.1 Selective ^{13}C signal excitation of the component with the longest ^{1}H T_{1rho} in a mixture

Figure 1 shows the pulse sequence for the selective ^{13}C signal excitation of the component with the longest ^{1}H T_{1rho} in the mixture (RFS method for long ^{1}H T_{1rho}). RF pulse for spin-locking was added to the pulse sequence of CP-MAS before the CP step. The method uses the decay of proton magnetization proceeding to null by

changing the spin-lock time, which enables the selective excitation of the ^{13}C signals of the component with the longest ^{1}H T_{1rho} in the mixture.

This sequence was subsequently applied to Saridon® Ace, which contains 250 mg of ethenzamide, 110 mg of acetaminophen, 100 mg of bromovalerylurea, 25 mg of caffeine, and 54 mg of excipients. Figure 2a shows the standard ^{13}C CP-MAS spectrum of Saridon® Ace. Carbon 13 signals corresponding to each active pharmaceutical ingredient and excipient were observed except for caffeine, which was formulated at the lowest concentration. The pulse sequence in Figure 1 was applied to Saridon® Ace, and the ^{13}C signals of ethenzamide in the mixture were selectively excited without the ^{13}C signals of acetaminophen or bromovalerylurea, as shown in Figure 2b. Compared with the standard ^{13}C CP-MAS spectra of Saridon® Ace shown in Figure 2a and ethenzamide shown in Figure 2c, the spectrum of ethenzamide in Saridon® Ace shown in Figure 2b was considered to be successfully extracted from the whole spectrum of Saridon® Ace.

The RFS method for long ^{1}H T_{1rho} is useful in the selective ^{13}C signal excitation of the component with the longest ^{1}H T_{1rho} in a mixture as the method utilizes the difference in ^{1}H T_{1rho} of each component and the decay of proton magnetization proceeding to null.

As previously Munson's group reported, carbon 13 signals of the longest ^{1}H T_{1rho} component in the mixture are able to be selectively excited via standard ^{13}C CP-MAS experiments with an extended contact time, as the magnetization of the short ^{1}H T_{1rho} components decays to null.[31] Such methodology is based on the magnetization decay related to ^{1}H T_{1rho} accompanied by cross-polarization. However, the NMR spectral profile at the optimal contact time differs from that at an extended contact time in this method, because cross-polarization efficiency is not unique to individual components.

As such, this method would be unable to extract an accurate spectral profile of individual components in a mixture. In contrast, the selective excitation of ^{13}C signals using the selective signal excitation method for long ^{1}H T_{1rho} was able to obtain an NMR spectral profile identical to those obtained in standard ^{13}C CP-MAS experiments, as this method uses a relatively long spin-lock time rather than extended contact time and the cross-polarization after spin-locking with optimal contact time was performed under the same conditions as the standard ^{13}C CP-MAS experiments.

A preliminary measurement was performed to optimize the length of τ delay in the pulse sequence of Figure 1 by plotting the correlation between the τ delay and signal intensity, usually using the pure compounds individually (e.g. crystals or amorphous). This was done using a two-dimensional NMR experiment which was expanded from the RFS method for long ^{1}H T_{1rho}, and utilizes the difference in ^{1}H T_{1rho} of each component and the decay of proton magnetization proceeding to null.

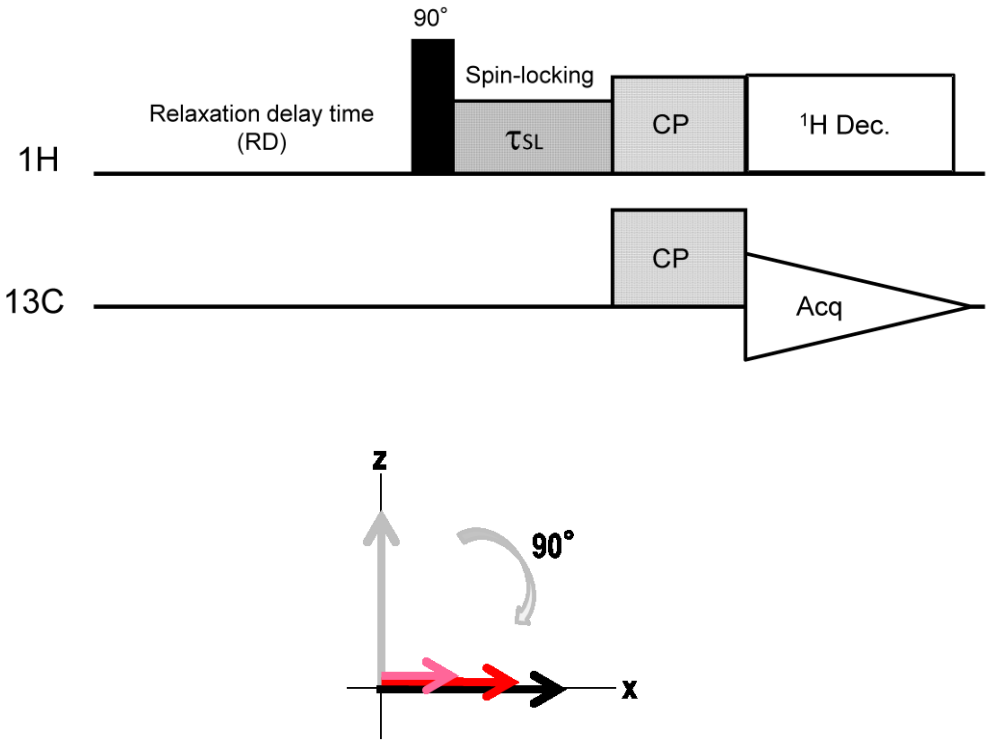

Figure 1. Pulse sequence and vector diagram for the selective ^{13}C signal excitation of the component with the longest ^{1}H T_{1rho} in a mixture (RFS method for long ^{1}H T_{1rho}).

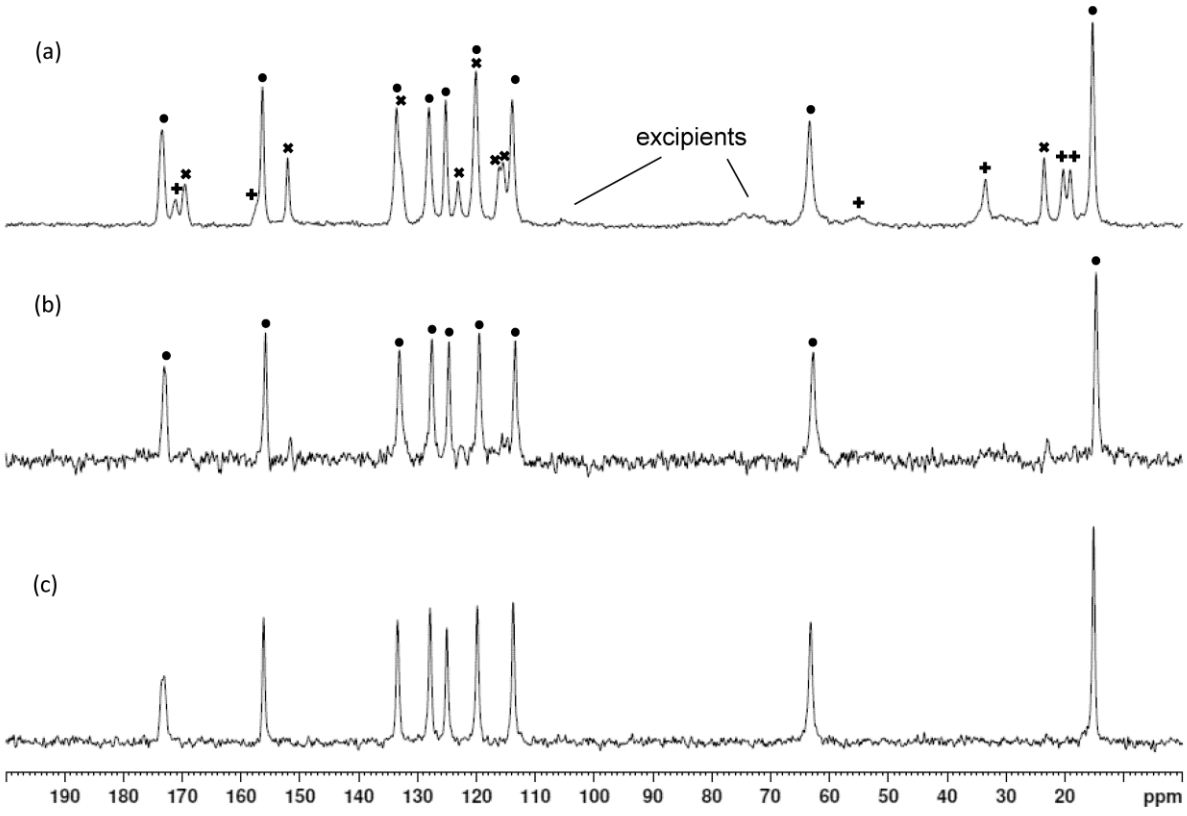

Figure 2. Solid state ^{13}C NMR spectra of Saridon® Ace (Daiichi Sankyo Company, Ltd.) and ethenzamide. (a) Standard ^{13}C CP-MAS spectrum of Saridon® Ace (Daiichi Sankyo Company, Ltd.) (•: ethenzamide, ×: acetaminophen, +: bromovalerylurea). (b) Selective ^{13}C signal excitation of ethenzamide (RFS method for long ^{1}H T_{1rho}) in Saridon® Ace (Daiichi Sankyo Company, Ltd.). (c) Standard ^{13}C CP-MAS spectrum of ethenzamide.

1.2 Application to quantitative analysis of crystallinity and polymorphs using the RFS method for long ^{1}H T_{1rho}

The author applied the RFS method for long ^{1}H T_{1rho} to the quantitative analysis of crystallinity for a physical mixture of crystals and amorphous solid dispersion of nifedipine with PVP K-30. The ^{13}C CP-MAS NMR spectra of 50% crystalline nifedipine with 30% PVP K-30, amorphous solid dispersion of nifedipine with 30% PVP K-30, and crystalline nifedipine are shown in Figure 3. The signal overlap between the ^{13}C signals from the crystalline and amorphous phases was observed in Figure 3. By applying the RFS method for long ^{1}H T_{1rho} at a relatively long spin-lock time (150 ms) with low spin-locking power (40.6 kHz) and a relaxation delay time (RD) of 50 s, ^{13}C signals of crystalline nifedipine with longer ^{1}H T_{1rho} than in the amorphous phases were selectively excited (Figure 3b). The author ensured the reliability of measurements of mixed phases by using an internal standard. Given that the author noted no overlap of the signals from acetaminophen with those of crystalline nifedipine on the high-field side, the author employed acetaminophen as an internal standard. The author used signals at 18.9, 35.2, 49.0, and 50.8 ppm for crystalline nifedipine and a signal at 23.2 ppm for acetaminophen for standard curves. The relative integrated intensity of each signal of crystalline nifedipine was calculated against the signal of acetaminophen and plotted against the crystallinity of nifedipine (Figure 4). The results of quantitative analysis of crystallinity are presented in Table 1 together with the results using 15% PVP K-30 and 20% PVP K-30 for amorphous solid dispersion of nifedipine.

The RFS method for long ^{1}H T_{1rho} was also applied to the quantitative analysis of a polymorphic mixture of indomethacin α form and γ form. The ^{13}C CP-MAS NMR

spectrum of a 50:50 polymorphic mixture of indomethacin α form and γ form showed the signal overlap between ^{13}C signals from the indomethacin α form and γ form (Figure 5a). By applying the RFS method for long ^{1}H T_{1rho} to a 50:50 polymorphic mixture of indomethacin α form and γ form, ^{13}C signals of indomethacin α form with a longer ^{1}H T_{1rho} than the γ form were selectively excited (Figure 5b). The relative integrated intensity of each signal of indomethacin α form was calculated against the signal of glycine (at 43.3 ppm or 176.0 ppm) as an internal standard and plotted against the quantitation of α form (Figure 6 and Figure 7). The results of quantitative analysis of α form in a 50:50 polymorphic mixture of indomethacin α form and γ form are presented in Table 2. The author was able to successfully obtain a quantitative value of the target component in a polymorphic mixture as well as the crystallinity of a partially amorphized drug substance.

As the RFS methods excite only the ^{13}C signals of the target component and give a less obstructive spectrum, they can be directly used in quantitative analysis of mixtures of different compounds, crystalline polymorphs, and mixtures of crystalline and amorphous forms of the same chemical compound without any mathematical adaptation, and would provide accurate estimation of the quantitative value of the target component. The author used the RFS method for long ^{1}H T_{1rho} for quantitation of crystallinity of a physical mixture of crystals and amorphous solid dispersion of nifedipine or quantitation of polymorphs in a polymorphic mixture of indomethacin α form, and γ form. However, the ^{1}H T_{1rho} of amorphous nifedipine or indomethacin γ form was too long and required a relatively long spin-lock time (>50 ms) to remove the signals. Typically, less than 50 ms of spin-lock time is used with high-power spin-locking, and thus a long duration with high-power irradiation could damage NMR systems, particularly probes and preamplifiers, which in turn means that the use of a

RFS method based on ^{1}H T_{1rho} under normal conditions would be difficult. The author used a long spin-lock time (150 ms) with low-power spin-locking (40.6 kHz) in the selective signal excitation method for long ^{1}H T_{1rho} to quantify the crystallinity of a physical mixture of crystals and amorphous solid dispersion of nifedipine or the polymorph of the α form in a polymorphic mixture of indomethacin α form and γ form. The results obtained in this manner allowed us to accurately determine the degree of quantitative value without any damage to the NMR system.

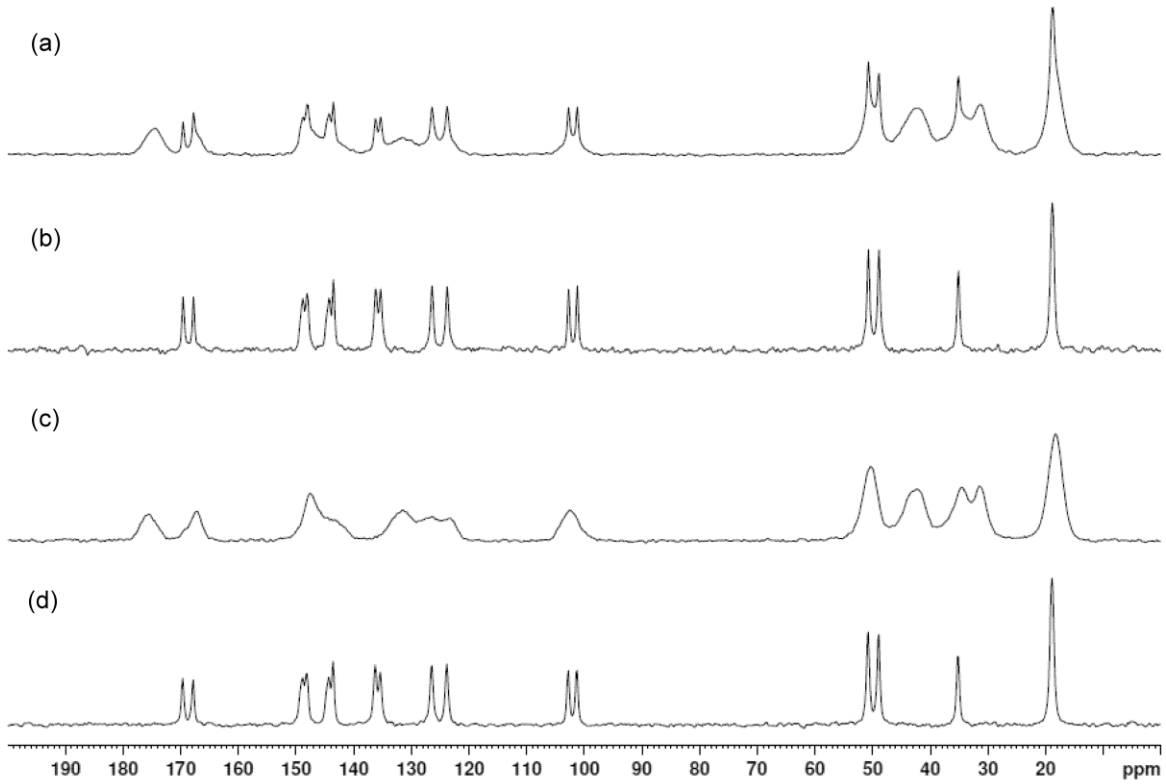

Figure 3. Solid state ^{13}C NMR spectra of nifedipine. (a) Standard ^{13}C CP-MAS spectrum of 50% crystalline nifedipine with 30% PVP K-30. (b) Selective ^{13}C signal excitation of crystalline nifedipine (RFS method for long ^{1}H T_{1rho}) in 50% crystalline nifedipine with 30% PVP K-30. (c) Standard ^{13}C CP-MAS spectrum of amorphous solid dispersion of nifedipine with 30% PVP K-30. (d) Standard ^{13}C CP-MAS spectrum of crystalline nifedipine.

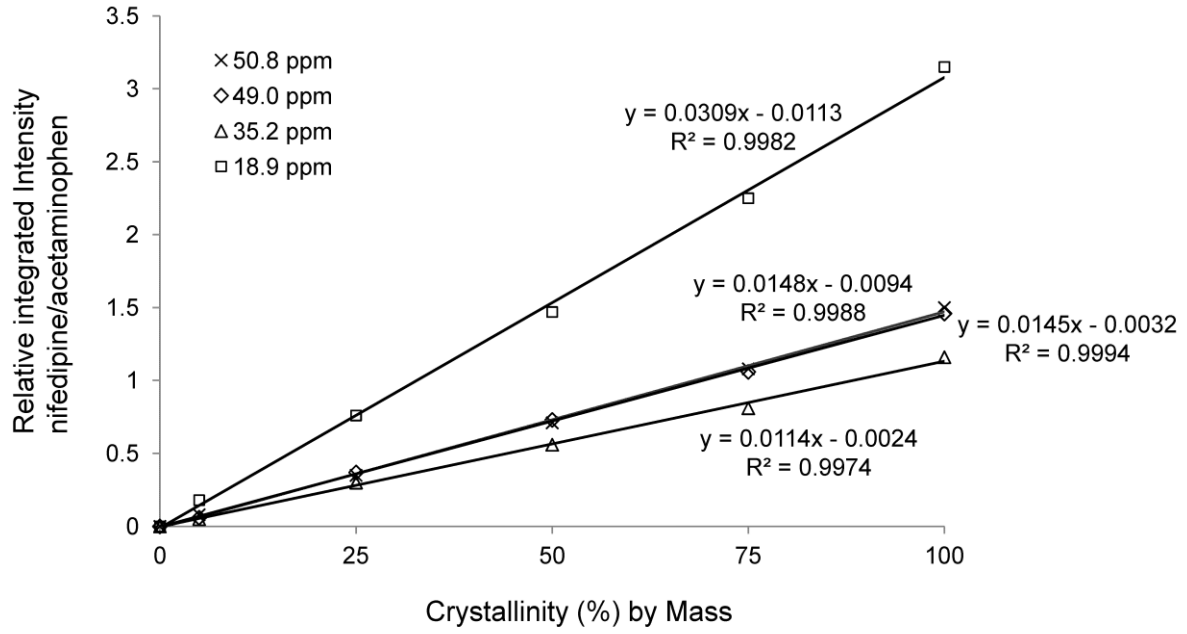

Figure 4. Relative integrated intensity versus crystallinity of nifedipine using a physical mixture of crystalline nifedipine and acetaminophen (signals at 18.9, 35.2, 49.0, and 50.8 ppm for crystalline nifedipine calculated against the signal at 23.2 ppm for acetaminophen).

Table 1. Results of quantitative analysis of crystallinity by ^{13}C NMR using the RFS method for long ^{1}H T_{1rho} for physical mixtures of 50% crystalline nifedipine with different ratios of PVP K-30

Percent-weight of PVP K-30	Crystallinity (%)				Average (%)
	50.8 ppm	49.0 ppm	35.2 ppm	18.9 ppm	
30	51	50	49	49	50
20	49	49	50	50	50
15	51	50	51	49	50

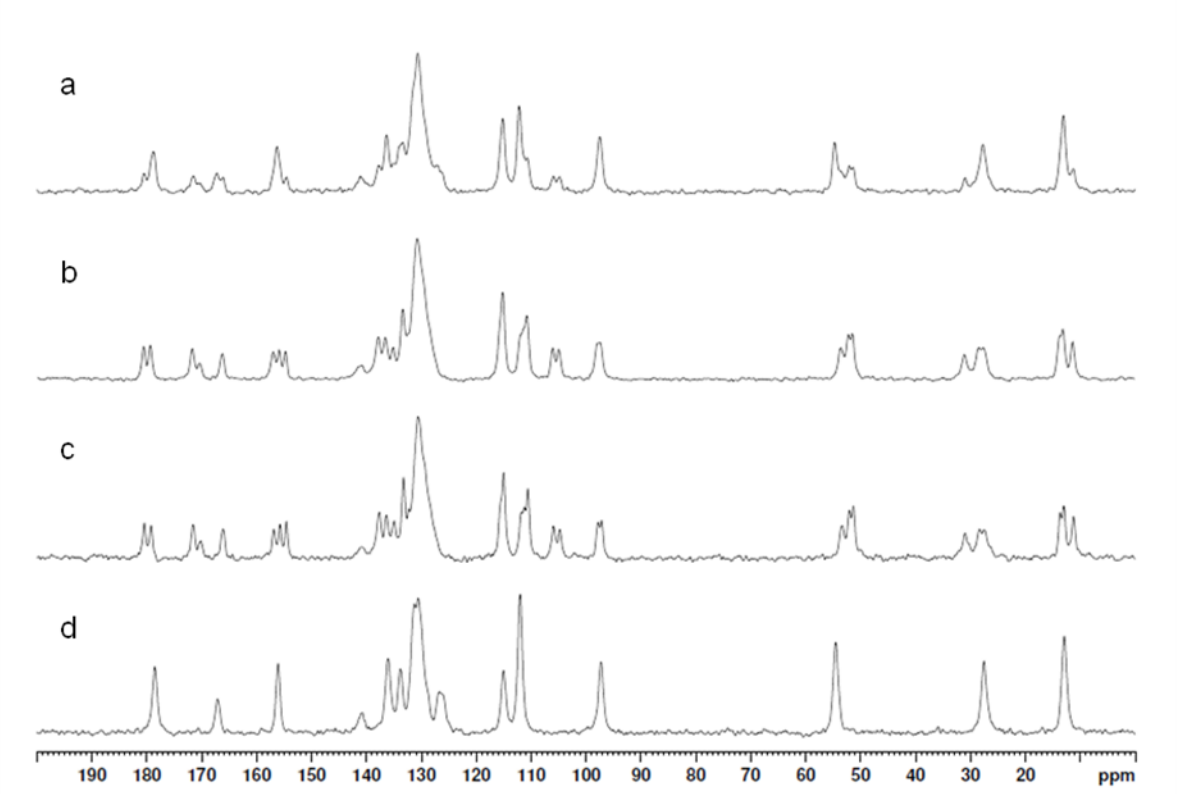

Figure 5. Solid state ^{13}C NMR spectra of indomethacin. (a) Standard ^{13}C CP-MAS spectrum of a 50:50 polymorphic mixture of indomethacin α-form and γ-form. (b) Selective ^{13}C signal excitation of indomethacin α-form (RFS method for long ^{1}H T_{1rho}) in a 50:50 polymorphic mixture of indomethacin α-form and γ-form. (c) Standard ^{13}C CP-MAS spectrum of indomethacin α-form. (d) Standard ^{13}C CP-MAS spectrum of indomethacin γ-form.

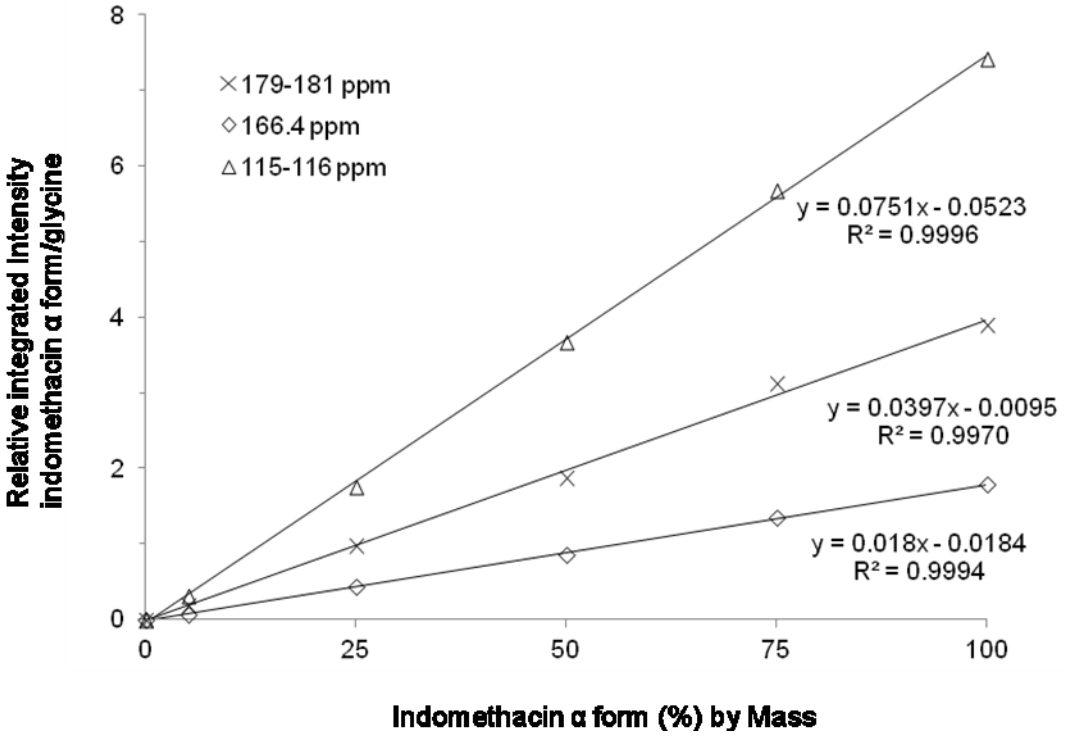

Figure 6. Relative integrated intensity vs. wt% by mass of indomethacin α-form using a physical mixture of indomethacin α-form and glycine (signals at 115-116, 166.4, 179-181 ppm for indomethacin α-form calculated against signal at 43.3 ppm for glycine).

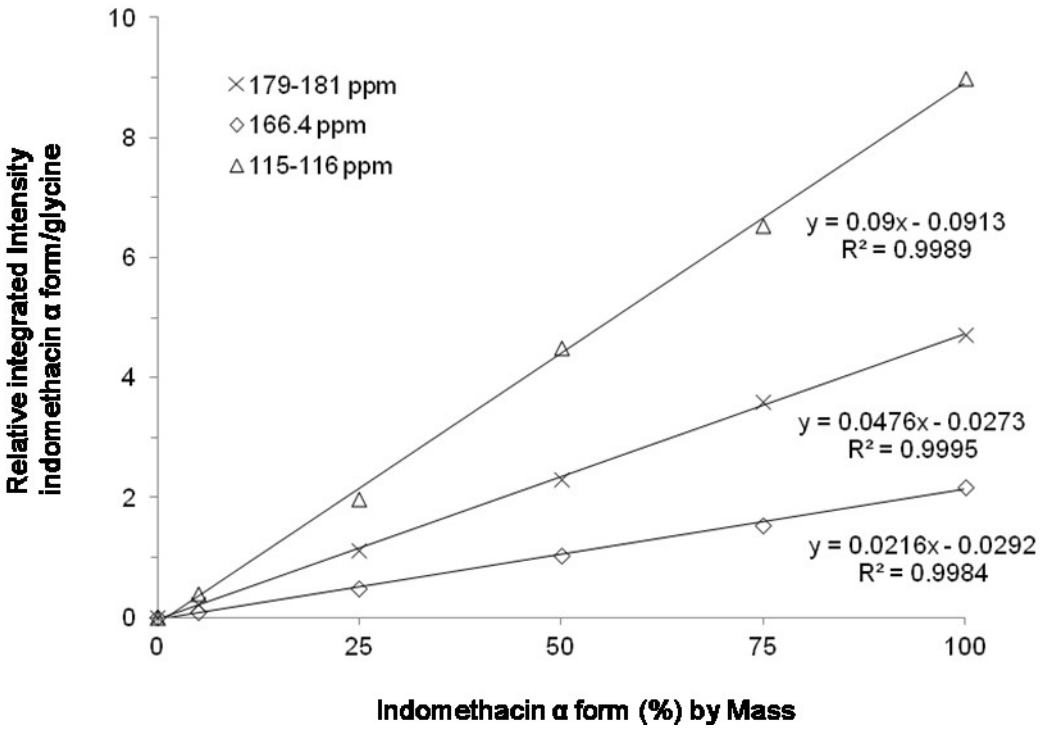

Figure 7. Relative integrated intensity vs. wt% by mass of indomethacin α-form using a physical mixture of indomethacin α-form and glycine (signals at 115-116, 166.4, 179-181 ppm for indomethacin α-form calculated against signal at 176.0 ppm for glycine).

Table 2. Results of quantitative analysis of a polymorph of α form in a 50:50 polymorphic mixture of indomethacin α form and γ form by ^{13}C NMR using the RFS method for long ^{1}H T_{1rho} with different signals of glycine as internal standard

Signals of glycine	Quantitation of α form (%)			Average (%)
	115-116 ppm	166.4 ppm	179-181 ppm	
43.3 ppm	49	50	52	50
176.0 ppm	51	50	52	51

1.3 Selective ^{13}C signal excitation of components with long or short ^{1}H T_{1rho} in a mixture

The RFS method for long ^{1}H T_{1rho} is used for selective ^{13}C signal excitation of the component with the longest ^{1}H T_{1rho} in a mixture. However, some mixtures consist of various components and have a number of different types of unique ^{1}H T_{1rho}. To selectively excite the ^{13}C signals of those components with long or short ^{1}H T_{1rho}, the author established an alternative method, which uses the difference between the two acquisitions obtained from the first pulse sequence, which includes a small-tip-angle RF pulse; and the second pulse sequence, which includes spin-locking before cross-polarization (RFS method for selective ^{1}H T_{1rho}).

The pulse sequence for the selective ^{13}C signal excitation of components with long or short ^{1}H T_{1rho} in a mixture (RFS method for selective ^{1}H T_{1rho}) is shown in Figure 8. The first pulse sequence had a small-tip-angle RF pulse (e.g. 30°, 60° RF pulse) instead of a 90° RF pulse and was followed by a second pulse sequence which included the spin-lock time before cross polarization. The difference between the first and the second free induction decay was then stored. Thus the method used proton magnetization from negative to positive which passes through null due to the difference in two acquisitions, which is useful in the selective ^{13}C signal excitation of components with long or short ^{1}H T_{1rho} in a mixture.

The applicability of this selective signal excitation method was demonstrated using a 1:1 mixture of α-lactose monohydrate and β-cyclodextrin (β-CD), and the results are presented in Figure 9. The standard ^{13}C CP-MAS spectrum of the mixture showed marked signal overlap between components due to the common portions of chemical structures between the saccharides (Figure 9a). Results of application of the pulse

sequence described in Figure 8 to the mixture are shown in Figure 9b and Figure 9d (the parameters listed in Table 3). As in Figure 9b, the ^{13}C signals of α-lactose monohydrate in the mixture were selectively excited, while none of β-CD were, and the same spectrum as the standard ^{13}C CP-MAS spectrum of α-lactose monohydrate shown in Figure 9c was obtained. In contrast, the ^{13}C signals of β-CD in the mixture were selectively excited with no α-lactose monohydrate signals as in Figure 9d, producing the same spectrum as the standard ^{13}C CP-MAS spectrum of β-CD shown in Figure 9e.

Using this method, the author was unable to gain maximum signal intensity as the author used a small-tip-angle RF pulse via acquisition of the first pulse sequence, while signal intensity via acquisition of the second pulse sequence decayed from maximum to null depending on the length of the spin-lock time. This finding indicates that the signals die out based on differences in signal intensity between the two acquisitions, which are subject to the selection of a suitable spin-lock time, and when the ^{13}C signals of one component are null, the ^{13}C signals of the other components will be excited in the negative or positive phase. Therefore, choosing a suitable spin-lock time facilitates the selective extraction of the spectrum of the target component with a short or long ^{1}H T_{1rho}.

When using the RFS method for selective ^{1}H T_{1rho} for selective signal excitation of components in a mixture with relatively long ^{1}H T_{1rho}, the efficiency of signal intensity can be increased by reducing the value of the small-tip-angle RF pulse in the first acquisition. For this reason, the ^{1}H magnetization of the second acquisition is amplified, as the ^{1}H magnetization of the component with long ^{1}H T_{1rho} decays slowly, and the ^{1}H magnetization of the first acquisition is decreased by reducing the value of the small-tip-angle. Thus, use of a suitable small-tip-angle allowed greater

^{1}H magnetization from the difference in the two acquisitions, allowing for effective achievement of signal intensity.

In contrast, for the selective ^{13}C signal excitation of a component in a mixture with a relatively short ^{1}H T_{1rho}, signal intensity efficiency was increased by expanding the value of the small-tip-angle RF pulse in the first acquisition. The ^{1}H magnetization of the second acquisition was thereby weakened, because the magnetization of components with relatively short ^{1}H T_{1rho} decays faster than that of components with longer ^{1}H T_{1rho}, whereas the greater ^{1}H magnetization of the first acquisition results can be achieved by expanding the value of the small-tip-angle. In short, greater ^{1}H magnetization can be obtained from the difference in the two acquisitions, allowing for effective achievement of signal intensity. Given the above findings regarding effective signal excitation of a mixture of α-lactose monohydrate and β-CD, the author used a reduced value for the small-tip-angle RF pulse (15°) for the selective ^{13}C signal excitation of α-lactose monohydrate, which has relatively long ^{1}H T_{1rho}, and expanded the value of the small-tip-angle RF pulse (60°) for the selective ^{13}C signal excitation of β-CD, which has relatively short ^{1}H T_{1rho}.

One advantage of this selective ^{13}C signal excitation by selective signal excitation method for long ^{1}H T_{1rho} and selective signal excitation method for selective ^{1}H T_{1rho} was that these methods were one-dimensional experiments. These methods therefore provide a considerable reduction in experimental duration compared with previously available approaches using inversion recovery or two-dimensional experiments. For example, only 5 min 21 s (16 scans, RD = 20 s) was spent using selective signal excitation method for long ^{1}H T_{1rho} in the selective excitation of ethenzamide in Saridon® Ace (Figure 2b), 5 h 2 min [360 scans, RD = 50 s, τ = 150 ms with low-power spin-locking (40.6 kHz)] for crystalline nifedipine in 50% crystallinity of

nifedipine with 30% w/w of PVP K-30 (30% PVP K-30) (Figure 3b), and 4 h 2 min [2160 scans, RD = 6.5 s, τ = 150 ms with low-power spin-locking (40.6 kHz)]) for indomethacin α-form in a 50:50 polymorphic mixture of indomethacin α-form and γ-form (Figure 5b), while 6 h 10 min (132 scans, RD = 84 s, τ = 7.84 ms) was spent using selective signal excitation method for selective $^{1}H\ T_{1rho}$ in the selective excitation of α-lactose monohydrate in a 1:1 mixture of α-lactose monohydrate and β-cyclodextrin (β-CD) (Figure 9b), and 5 h 42 min (640 scans, RD = 16 s, τ = 5 ms) for β-CD in a 1:1 mixture of α-lactose monohydrate and β-CD (Figure 9d). In contrast, the general experiment takes approximately 10 to 50 h for two-dimensional-based experiments (TOSY or ROSY) and from one to several days for inversion recovery-based experiments (DECRA).

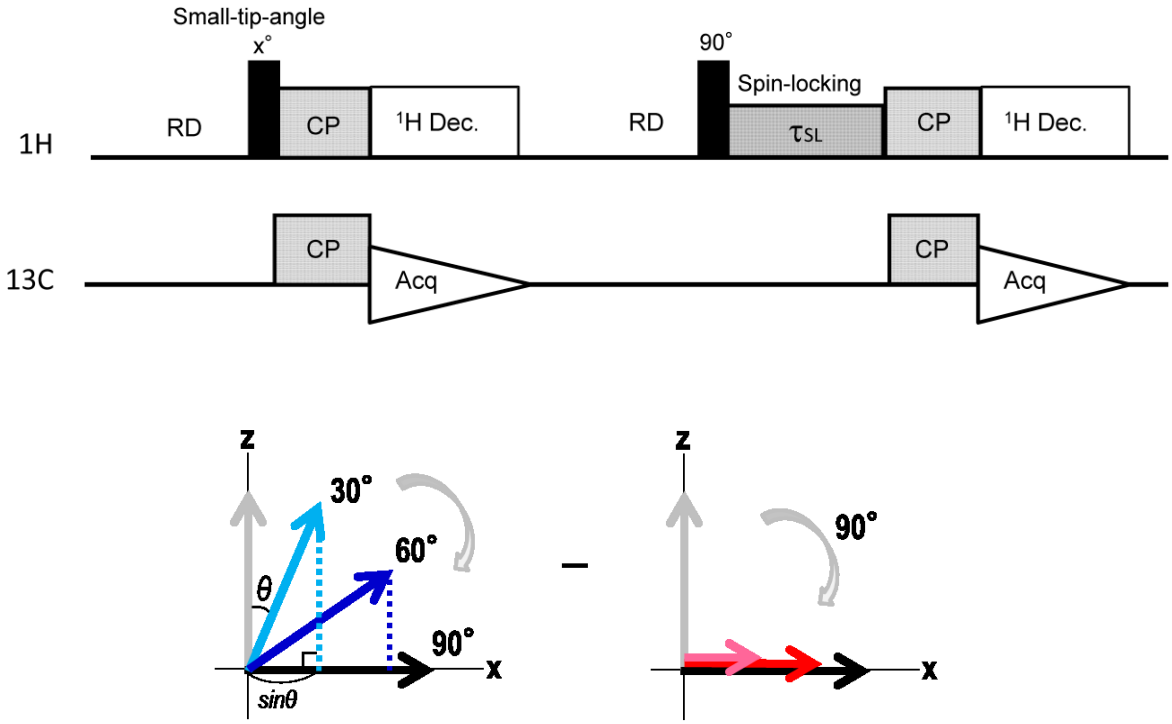

Figure 8. Pulse sequence and vector diagram for the selective ^{13}C signal excitation of components with long or short ^{1}H T_{1rho} in a mixture (RFS method for selective ^{1}H T_{1rho}).

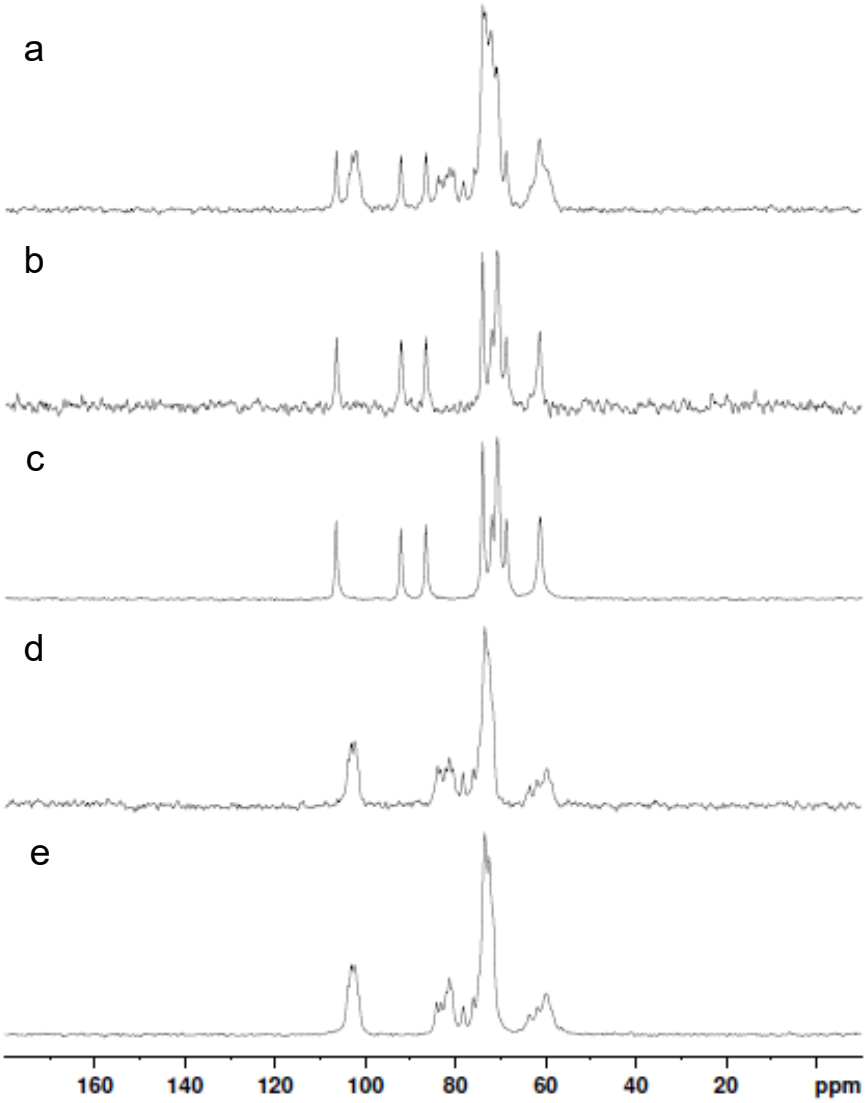

Figure 9. Solid state ^{13}C NMR spectra of the mixture and pure material of α-lactose monohydrate and β-CD. (a) Standard ^{13}C CP-MAS spectrum of the mixture of α-lactose monohydrate and β-CD. (b) Selective ^{13}C signal excitation of α-lactose monohydrate (RFS method for selective ^{1}H T_{1rho}) in the mixture. (c) Standard ^{13}C CP-MAS spectrum of α-lactose monohydrate. (d) Selective ^{13}C signal excitation of β-CD (RFS method for selective ^{1}H T_{1rho}) in the mixture. (e) Standard ^{13}C CP-MAS spectrum of β-CD.

Table 3. Experimental parameters for the mixture of α-lactose monohydrate and β-CD in the RFS method for selective ^{1}H T_{1rho}

Selectively excited	Small-tip-angle (degree)	τ_{SL} (msec)	RD (sec)
α-lactose monohydrate	15	7.84	84
β-CD	60	5.00	16

CHAPTER 2

The RFS methods for ^{1}H T_1 in ^{13}C solid state NMR spectroscopy

2.1 Selective ^{13}C signal excitation of the component with the longest ^{1}H T_1 in a mixture

RFS methods with ^{1}H T_{1rho} are useful for the extraction of signals of the target component. However, if each component in a mixture has the same or a similar ^{1}H T_{1rho}, a shift to RFS methods with ^{1}H T_1 would be expected. In the case of a physical mixture of crystalline α-lactose monohydrate and amorphous lactose, use of the RFS method using ^{1}H T_{1rho} was difficult because of the similar ^{1}H T_{1rho} (9.3 ms for crystalline α-lactose monohydrate and 8.3 ms for amorphous lactose). Given the difference between ^{1}H T_1 for crystalline α-lactose monohydrate (88 s) and amorphous lactose (3.9 s), the spectrum of the target component could be selectively extracted from the mixture using the RFS method for long ^{1}H T_1.

Figure 10 shows the pulse sequence for selective ^{13}C signal excitation of the component with the longest ^{1}H T_1 in the mixture (RFS method for long ^{1}H T_1). This sequence was subsequently applied to Saridon® Ace, which contains 250 mg of ethenzamide, 110 mg of acetaminophen, 100 mg of bromovalerylurea, 25 mg of caffeine anhydrous, and 54 mg of excipients. Figure 11a shows the standard ^{13}C CP-MAS spectrum of Saridon® Ace (RD=120 s). Carbon 13 signals corresponding

to each active pharmaceutical ingredient and excipient were observed except for caffeine anhydrous, which was formulated at the lowest concentration. A preliminary measurement was performed to optimize the length of τ delay in the pulse sequence of Figure 10 by plotting the correlation between the τ delay and signal intensity, usually using the pure compounds individually (e.g. crystals or amorphous). This was done using a two-dimensional NMR experiment which was expanded from the RFS method for long ^{1}H T_1 and required 0.5 to 6 h to optimize τ delay for each of the objective compounds. The total scan for each compound depended on the required signal-to-noise ratio. Figure 12a shows the correlation between the τ delay and signal intensity. The signal intensity of ethenzamide or bromovalerylurea with a shorter ^{1}H T_1 rapidly decreased, whereas that of acetaminophen with the longer ^{1}H T_1 slowly decreased as the relaxation proceeded. Given the above findings, the author successfully selectively excited the ^{13}C signals of acetaminophen, which had the longest ^{1}H T_1 in Saridon® Ace, without exciting the signals of the other components of this product using the RFS method for long ^{1}H T_1 with 45 s for both RD and τ delay (Figure 11b). On comparison with the standard ^{13}C CP-MAS spectra of Saridon® Ace (Figure 11a) and acetaminophen (Figure 11e), the spectrum of acetaminophen in Saridon® Ace (Figure 11b) was considered successfully extracted from the whole spectrum of Saridon® Ace.

The RFS method for long ^{1}H T_1 was also applied to a physical mixture of crystalline α-lactose monohydrate and amorphous lactose (Figure 13). Carbon 13

signals of crystalline α-lactose monohydrate, which has a longer ^{1}H T_1 than amorphous lactose, were successfully extracted from the mixture by setting RD at 84 s and τ delay at 30 s.

The author developed a new RFS method which utilizes the difference in ^{1}H T_1 of each component and the decay of proton magnetization proceeding to null, and succeeded in selective signal excitation of the component with the longest ^{1}H T_1 in a mixture. Selective excitation of signals from the component with the longest ^{1}H T_1 in a mixture using the normal ^{13}C CP pulse sequence or slightly modified sequences is not possible, because signal intensity increases as the excited signals return to the ground state with increasing RD. This limitation is based on the recovery of longitudinal magnetization, referred to as ^{1}H T_1, after a ^{1}H 90° radio frequency (RF) pulse irradiation.

This sequence uses two acquisition steps in the phase cycle. In the first acquisition step, the first (90°y) pulse flips the proton magnetization to the transverse plane (+x axis), and after a negligible delay the second (90°-y) pulse flips it back to the +z longitudinal axis. The τ delay then proceeds, and the proton magnetization goes back to its fully relaxed state along the longitudinal axis. The third (90°y) pulse flips the proton magnetization with the fully relaxed state to the transverse plane (+x axis) again, and then the NMR spectra are acquired. In the second acquisition step of the phase cycle, the first (90°y) pulse flips the proton magnetization to the transverse plane (+x axis), as in the first acquisition step of the phase cycle, and the second

(90°y) pulse flips it to the -z longitudinal axis. Recovery of the inverted magnetization along the longitudinal axis is followed using a (90°-y) pulse with the detection of signals on the +x axis at a short length of τ delay. The proton magnetization passes through null and signal detection on the -x axis occurs as the length of the τ delay increases, which induces the decay of the inverted magnetization along the longitudinal axis. The addition of the first and second acquisition steps of the phase cycle allows various signal intensities to be obtained. Thus, this method utilizes the difference in ^{1}H T_1 of each component and the decay of proton magnetization proceeding to null.

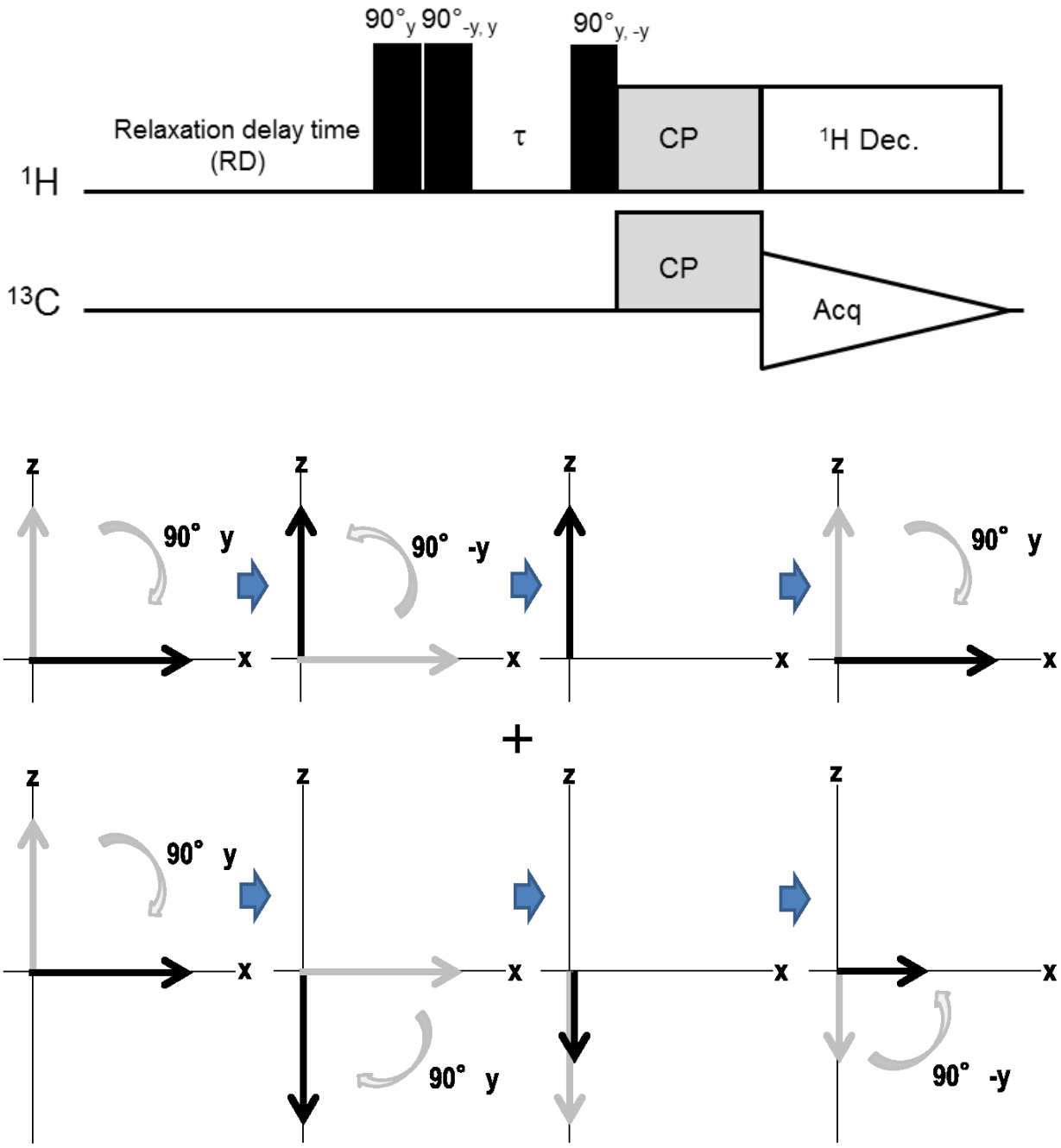

Figure 10. Pulse sequence and vector diagram for the selective ^{13}C signal excitation of the component with the longest ^{1}H T_1 in a mixture (RFS method for long ^{1}H T_1).

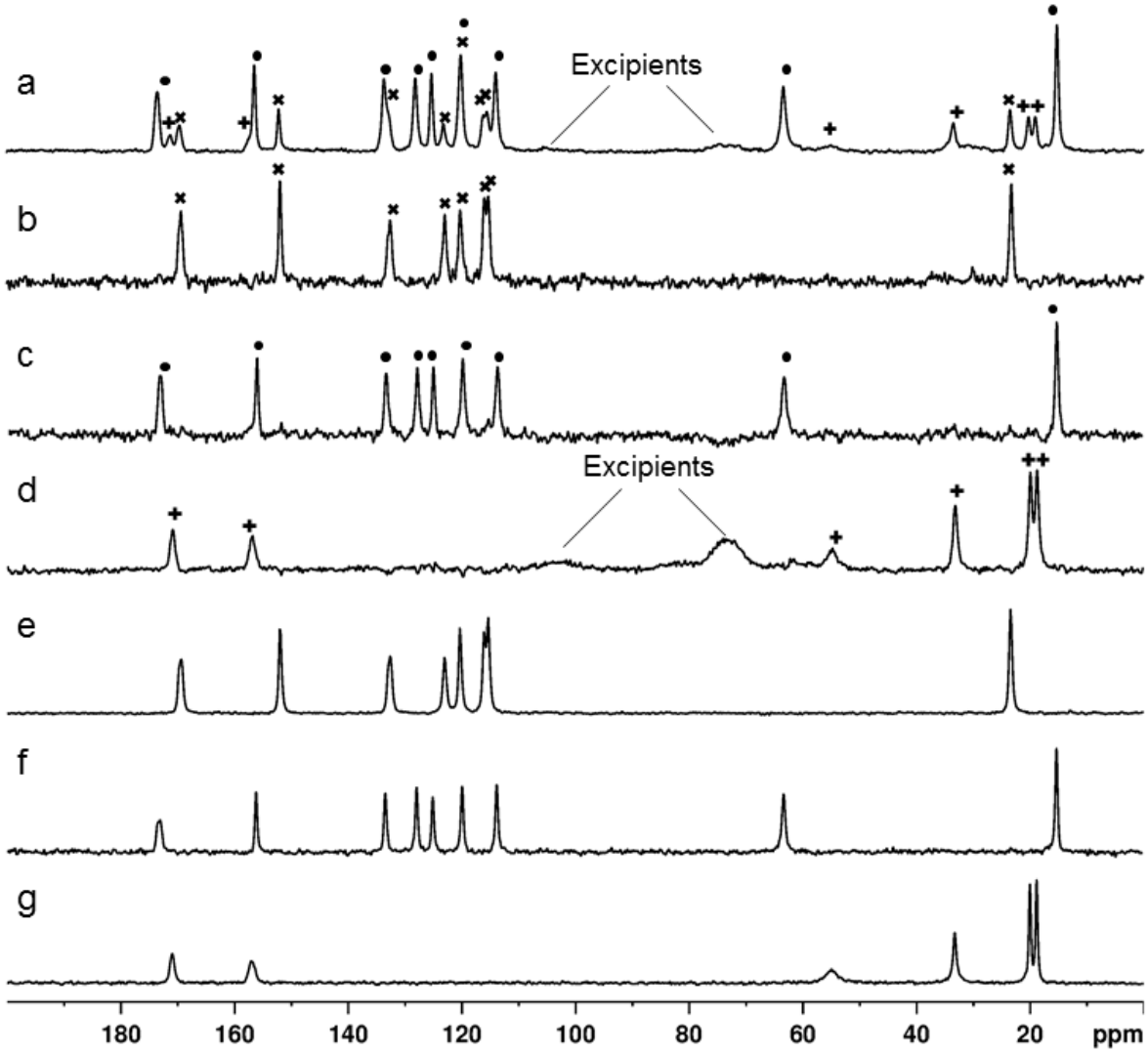

Figure 11. Solid state ^{13}C NMR spectra of Saridon® Ace and reference standards. (a) Standard ^{13}C CP-MAS spectrum of Saridon® Ace (•: ethenzamide, ×: acetaminophen, +: bromovalerylurea). (b) Selective ^{13}C signal excitation of acetaminophen (RFS method for long ^{1}H T_1) in Saridon® Ace. (c) Selective ^{13}C signal excitation of ethenzamide (RFS method for selective ^{1}H T_1) in Saridon® Ace. (d) Selective ^{13}C signal excitation of bromovalerylurea (RFS method for selective ^{1}H T_1) in Saridon® Ace. (e) Standard ^{13}C CP-MAS spectrum of acetaminophen. (f) Standard ^{13}C CP-MAS spectrum of ethenzamide. (g) Standard ^{13}C CP-MAS spectrum of bromovalerylurea.

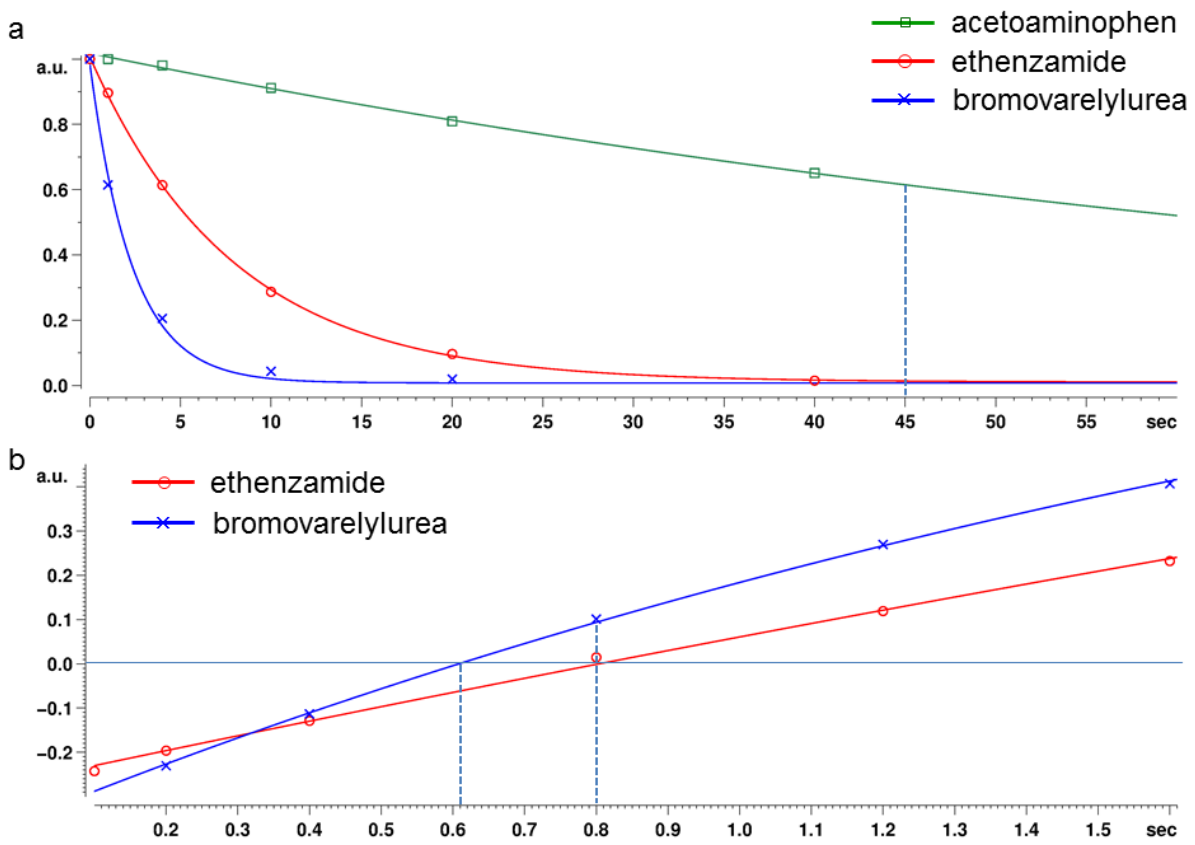

Figure 12. The correlation between the signal intensity versus τ delay using RFS methods for Saridon® Ace. (a) RFS method for long ^{1}H T_1. (b) RFS method for selective ^{1}H T_1 (RD=1 s). Dot lines are optimized for τ delay for each RFS method.

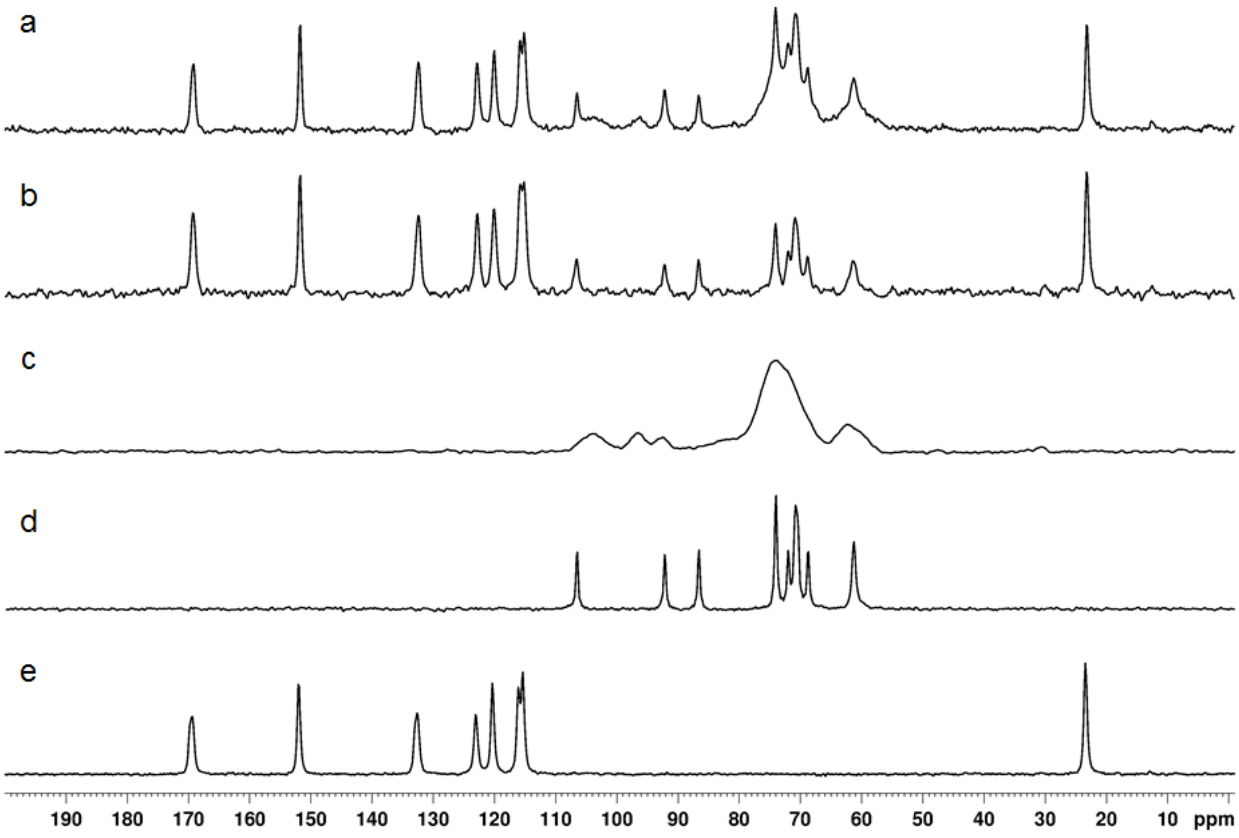

Figure 13. Solid state ^{13}C NMR spectra of lactose and acetaminophen. (a) Standard ^{13}C CP-MAS spectrum of a 50:50 mixture of α-lactose monohydrate and amorphous lactose with acetaminophen. (b) Selective ^{13}C signal excitation of α-lactose monohydrate with acetaminophen (RFS method for long ^{1}H T_1) in a 50:50 mixture of α-lactose monohydrate and amorphous lactose with acetaminophen. (c) Standard ^{13}C CP-MAS spectrum of amorphous lactose. (d) Standard ^{13}C CP-MAS spectrum of α-lactose monohydrate. (e) Standard ^{13}C CP-MAS spectrum of acetaminophen.

2.2 Application to quantitative analysis of crystallinity using RFS method for long ^{1}H T_1

The author applied the RFS method for long ^{1}H T_1 to the quantitative analysis of crystallinity for a physical mixture of crystalline nifedipine and amorphous solid dispersion of nifedipine with PVP K-30. Figure 14a shows the signal overlap between the ^{13}C signals from the crystalline and amorphous phases. By applying the RFS method for long ^{1}H T_1, ^{13}C signals of crystalline nifedipine with longer ^{1}H T_1 than in the amorphous phases were selectively excited (Figure 14b). The author ensured the reliability of measurements of mixed phases by using acetaminophen as an internal standard. Signals which did not overlap between acetaminophen and crystalline nifedipine were used for standard curves, namely those at 18.9, 35.2, 49.0, and 50.8 ppm for crystalline nifedipine and at 23.2 ppm for acetaminophen. The relative integrated intensity of each signal of crystalline nifedipine was calculated against the signal of acetaminophen and plotted against the crystallinity of nifedipine (Figure 15). The results of quantitative analysis of crystalline nifedipine are presented in Table 4.

Furthermore, the author applied the RFS method for long ^{1}H T_1 to the 5% crystallinity of nifedipine with 30% PVP K-30 to confirm low-level crystalline content detection, and succeeded in selective signal excitation of the crystalline phase (Figure 14c).

The author also quantitatively analyzed crystallinity for α-lactose monohydrate in mixtures of α-lactose monohydrate and amorphous lactose mixed in various ratios. The author used the signals at 61.3, 86.7, and 106.5 ppm for α-lactose monohydrate and a signal at 23.2 ppm for acetaminophen. The relative integrated intensity of each signal of α-lactose monohydrate was calculated against the signal of acetaminophen

and plotted against the crystallinity of α-lactose monohydrate (Figure 16). Crystallinities for α-lactose monohydrate were accurately determined as in Table 5.

Because the RFS methods excite only the ^{13}C signals of the target component and provide a less obstructive spectrum, they can be used directly in the quantitative analysis of mixtures of different compounds, crystalline polymorphs, and mixtures of crystalline and amorphous forms of the same chemical compound without any mathematical adaptation, and allow the quantitative value of the target component to be accurately estimated.

The author applied the RFS method for long ^{1}H T_1 to quantify the crystallinity of physical mixtures of crystals and amorphous solid dispersion of nifedipine with various ratios of PVP K-30 or crystallinity of physical mixtures with various proportions of crystalline α-lactose monohydrate and amorphous lactose. Any signal can be used for these quantitative analyses because all the signals of crystalline nifedipine and crystalline α-lactose monohydrate used for standard curves showed good linearity (Figure 15 and Figure 16). The author accurately obtained the crystallinity of crystalline nifedipine in a physical mixture of 50% crystalline nifedipine in solid dispersion with various ratios of PVP K-30, and showed that quantitation was not affected by the ratios of PVP K-30 in solid dispersion in the range of 15% to 30% (Table 4). Additionally, quantitative analysis of crystalline α-lactose monohydrate in physical mixtures with various proportions of crystalline α-lactose monohydrate and amorphous lactose was successfully established (Table 5).

However, the finding that domain size of the averaged ^{1}H T_1 is in the range of several tens of nanometers indicates that some crystalline compounds may not have a constant ^{1}H T_1 for reasons such as crystal defect.[32] Preparation of standard curves in highly accurate quantitation of crystallinity should therefore be done using high

crystallinity compounds. For quantitation of mixtures of different compounds or crystalline polymorphs, it would be better to use a material which has a similar ^{1}H T_1 to the standard curve or to use other RFS methods (e.g. RFS method for long ^{1}H T_{1rho} or RFS method for selective ^{1}H T_{1rho}, whose effective domain size is in the quite small range of several nanometers), with sufficient recycle delay time for accurate quantitation.

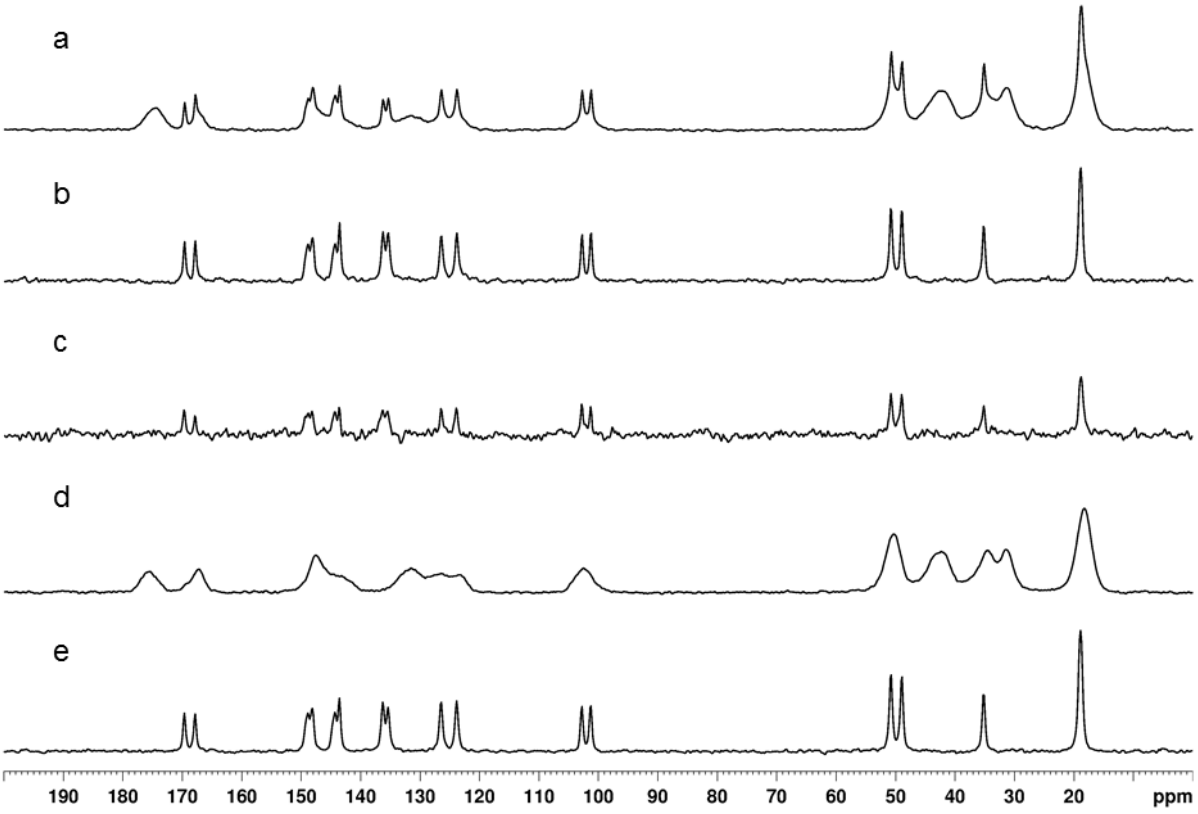

Figure 14. Solid state ^{13}C NMR spectra of nifedipine. (a) Standard ^{13}C CP-MAS spectrum of 50% crystallinity of nifedipine with 30% PVP K-30. (b) Selective ^{13}C signal excitation of crystalline nifedipine (RFS method for long ^{1}H T_1) in 50% crystallinity of nifedipine with 30% PVP K-30. (c) Selective ^{13}C signal excitation of crystalline nifedipine (RFS method for long ^{1}H T_1) in 5% crystallinity of nifedipine with 30% PVP K-30. (d) Standard ^{13}C CP-MAS spectrum of amorphous solid dispersion of nifedipine with 30% PVP K-30. (e) Standard ^{13}C CP-MAS spectrum of crystalline nifedipine.

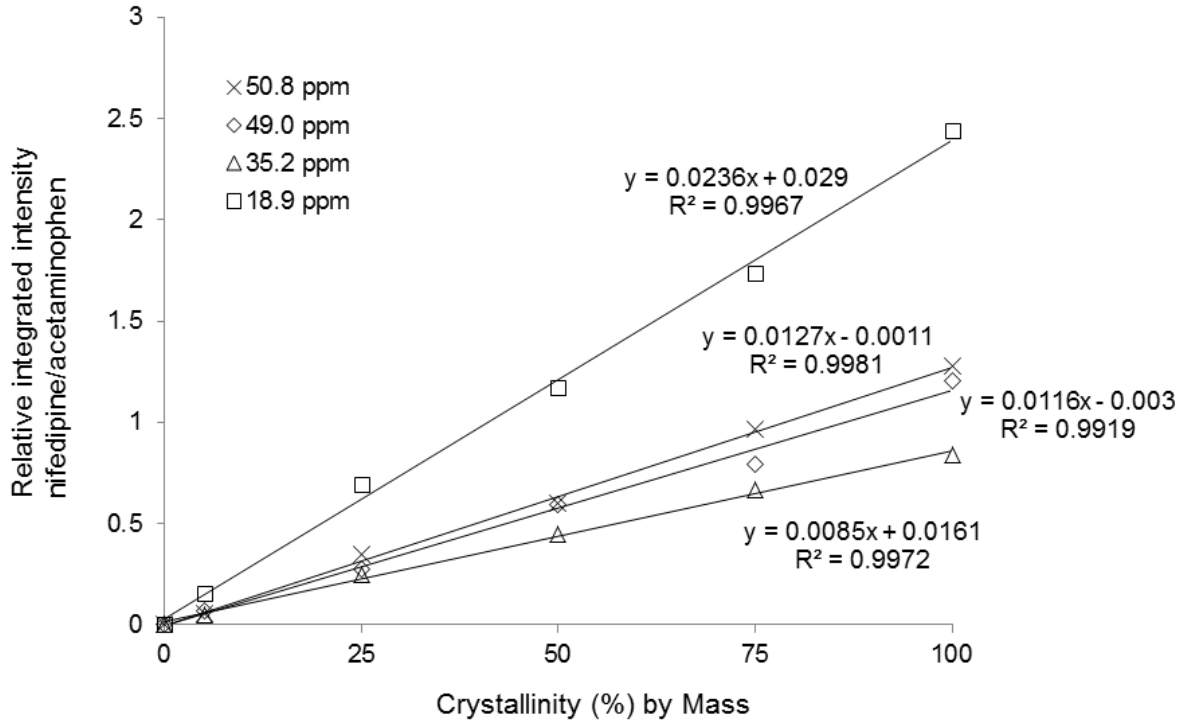

Figure 15. Relative integrated intensity versus crystallinity of nifedipine using a physical mixture of crystalline nifedipine and acetaminophen (signals at 18.9, 35.2, 49.0 and 50.8 ppm for crystalline nifedipine calculated against the signal at 23.2 ppm for acetaminophen).

Table 4. Quantitative analysis of crystallinity by 13C NMR using the RFS method for long ^{1}H T_1 for physical mixtures of 50% crystalline nifedipine with different ratios of PVP K-30

Percent-weight of PVP K-30	Crystallinity (%)				Average (%)
	50.8 ppm	49.0 ppm	35.2 ppm	18.9 ppm	
30	48	51	51	48	50
20	47	48	49	49	48
15	49	50	51	51	50

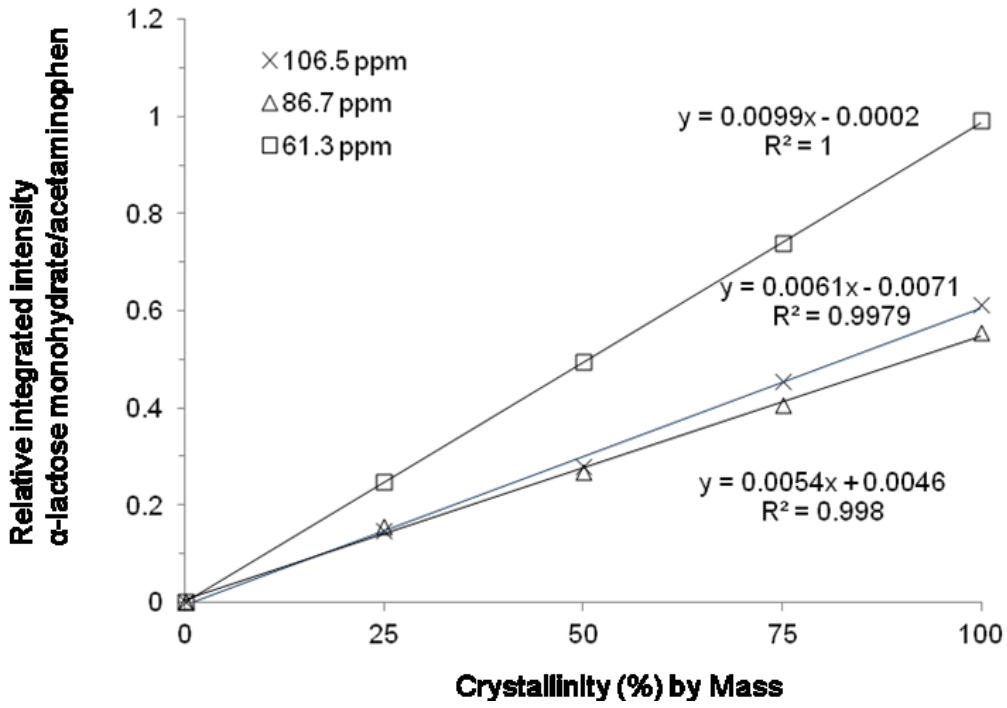

Figure 16. Relative integrated intensity versus crystallinity of α-lactose monohydrate using a physical mixture of α-lactose monohydrate and acetaminophen (signals at 61.3, 86.7 and 106.5 ppm for crystalline nifedipine calculated against the signal at 23.2 ppm for acetaminophen).

Table 5. Quantitative analysis of crystallinity by ^{13}C NMR using the RFS method for long ^{1}H T_1 for physical mixtures of different ratios of crystalline α-lactose monohydrate and amorphous lactose

Percent-weight of α-lactose monohydrate	Crystallinity (%)			Average (%)
	106.5 ppm	86.7 ppm	61.3 ppm	
75	73	75	75	75
50	51	50	50	50
25	25	25	26	25

2.3 Selective ^{13}C signal excitation of components with long or short ^{1}H T_1 in a mixture and application to quantitative analysis of polymorphs

The pulse sequence for the selective ^{13}C signal excitation of components with long or short ^{1}H T_1 in a mixture (RFS method for selective ^{1}H T_1) is shown in Figure 17. This RFS method was applied to Saridon® Ace. The spectra of ethenzamide (Figure 11c) and bromovalerylurea (Figure 11d) were individually extracted from the whole spectrum of Saridon® Ace, and the same spectrum as the standard ^{13}C CP-MAS spectrum of ethenzamide (Figure 11f) and bromovalerylurea (Figure 11g) was obtained. A preliminary measurement was performed to optimize the length of τ delay in the pulse sequence of Figure 17 by plotting the correlation between the τ delay and signal intensity. To do this the author used the pulse sequence of the inversion recovery (180°–τ–90°) with CP in the 2D NMR experiment.[33] Figure 12b shows the correlation between τ delay and signal intensity using the pulse sequence of Figure 17 for Saridon® Ace with RD in 1 s. Null points of bromovalerylurea (0.61 s) and ethenzamide (0.80 s) were optimized for the detection of each targeted compound.

The RFS method for selective ^{1}H T_1 was also applied to a polymorphic mixture of bromovalerylurea Form I and Form II (Figure 18). The ^{13}C signals of bromovalerylurea Form I in the mixture were selectively excited (Figure 18b), whereas those of bromovalerylurea Form II were not, by setting the condition under which the Form II signal intensity became null. The same spectrum as the standard ^{13}C CP-MAS spectrum of bromovalerylurea Form I was obtained (Figure 18d). In the same way, the ^{13}C signals of bromovalerylurea Form II in the mixture were selectively excited (Figure 18c), producing the same spectrum as the standard ^{13}C CP-MAS

spectrum of bromovalerylurea Form II (Figure 18e) by setting the condition under which the Form I signal intensity became null.

The author used a 35:65 polymorphic mixture of bromovalerylurea Form I and Form II for quantitative analysis using the RFS method for selective ^{1}H T_1. The author used the signals at 17.8–20.8, 33.4 and 157.0 ppm for bromovalerylurea Form I and a signal at 26.5 ppm for sodium acetate. The relative integrated intensity of each signal of bromovalerylurea Form I was calculated against the signal at 26.5 ppm for sodium acetate as an internal standard and plotted against the quantitation of Form I (Figure 19a). The results of quantitative analysis of Form I in a 35:65 polymorphic mixture of bromovalerylurea Form I and Form II are presented in Table 6a. The author used the signals at 20.6, 33.0 and 170.5 ppm for bromovalerylurea Form II and a signal at 43.3 ppm for glycine. The relative integrated intensity of each signal of bromovalerylurea Form II was calculated against the signal of glycine as an internal standard and plotted against the quantitation of Form II (Figure 19b). The results of quantitative analysis of Form II in a 35:65 polymorphic mixture of bromovalerylurea Form I and Form II are presented in Table 6b. The author successfully obtained a quantitative value of the target component in a polymorphic mixture.

The RFS method for selective ^{1}H T_1 can selectively excite the ^{13}C signals of those components with long or short ^{1}H T_1, or in other words extract the individual spectrum of various components.

The sequence uses a 180° pulse to place the proton magnetization to the -z axis. Decay of the inverted magnetization along the longitudinal axis is followed using a (90°y) pulse which flips the proton magnetization to the transverse plane (-x axis) at a short length of τ delay with the detection as negative signals. After the proton magnetization on the +z axis passes through null with an increase in the length of

τ delay, the decay of the inverted magnetization that returns to its ground state is followed using a (90°y) pulse to place the proton magnetization to the +x axis, with detection as a positive signal.

Thus, the method provides for the transition of proton magnetization from negative to positive, which passes through null. The component with the shorter ^{1}H T_1 recovers signal intensity rapidly while the component with the longer ^{1}H T_1 recovers signal intensity slowly, as relaxation proceeds. It follows that ^{13}C signals of the target component are selectively excited under conditions in which the other component does not give signal intensity.

The author applied this method to Saridon® Ace, which contains more than two components. Despite the difficulty of applying this method to mixtures of more than two components, the author successfully selectively extracted the ^{13}C signals of two individual components separately by saturating the ^{13}C signals of acetaminophen, which has a long ^{1}H T_1 (110 s), using a short RD (1 s). This RFS method for selective ^{1}H T_1 was then applied and the ^{13}C signals of ethenzamide or bromovalerylurea were selectively excited by setting the condition under which the other signal intensity became null (Figure 12b). The ^{1}H T_1 of excipients was almost the same as that of bromovalerylurea, which was selectively extracted from Saridon® Ace (Figure 11d), but the signals of bromovalerylurea and excipients did not overlap.

The author was able to selectively extract all three components in Saridon® Ace separately using the RFS method for long ^{1}H T_1 for acetaminophen and the RFS method for selective ^{1}H T_1 for ethenzamide and bromovalerylurea. As in this case, the author are able to selectively extract each component from a mixture which had more than two components using four different types of RFS method, namely the RFS

method for long ^{1}H T_1, the RFS method for selective ^{1}H T_1, the RFS method for long ^{1}H T_{1rho} and the RFS method for selective ^{1}H T_{1rho}.

The author also used the RFS method for selective ^{1}H T_1 to quantify polymorphs in a polymorphic mixture of bromovalerylurea Form I and Form II. In this study, although the difference in ^{1}H T_1 between Form I (1.8 s) and Form II (1.1 s) was small, the individual spectrum of each component was successfully extracted from the mixture (Figure 18). All signals of bromovalerylurea Form I and Form II used for the standard curve showed good linearity (Figure 19). The author was able to accurately determine the quantitative value of both bromovalerylurea Form I or Form II in the 35:65 polymorphic mixture (Table 6). For selection of the internal standards in quantitative analysis, the author selected those that had to be detected at the same phase as the targeted component under the experimental conditions of each RFS method. For example, the author selected sodium acetate, which has a long ^{1}H T_1 (32 s), for quantitative analysis of bromovalerylurea Form I, which has a longer ^{1}H T_1 than Form II; and glycine, which has a shorter ^{1}H T_1 (0.3 s), for quantitative analysis of bromovalerylurea Form II, which has a shorter ^{1}H T_1 than Form I.

The RFS methods using ^{1}H T_1 are simple as they are one-dimensional experiments as the RFS methods using ^{1}H T_{1rho}, they provide a considerable reduction in experimental duration compared to the existing methods using inversion recovery or two-dimensional experiments. For example, selective signal excitation of crystalline nifedipine in 50% crystallinity of nifedipine with 30% w/w of PVP K-30 (30% PVP K-30) using the RFS method for long ^{1}H T_1 required 9 h 15 min (512 scans, RD = 50 s, τ = 15 s) (Figure 14b), and selective signal excitation of α-lactose monohydrate with acetaminophen in a 50:50 mixture of α-lactose monohydrate and amorphous lactose with acetaminophen using the RFS

method for long ^{1}H T_1 required 5 h 4 min (160 scans, RD = 84 s, τ = 30 s) (Figure 13b). For selective signal excitation of bromovalerylurea Form I and Form II in a 35:65 polymorphic mixture using the RFS method for selective ^{1}H T_1, bromovalerylurea Form I required 1 h 30 min (800 scans, RD = 6 s, τ = 0.71 s) (Figure 18b), while bromovalerylurea Form II required 1 h 34 min (800 scans, RD = 6 s, τ = 1.03 s) (Figure 18c).

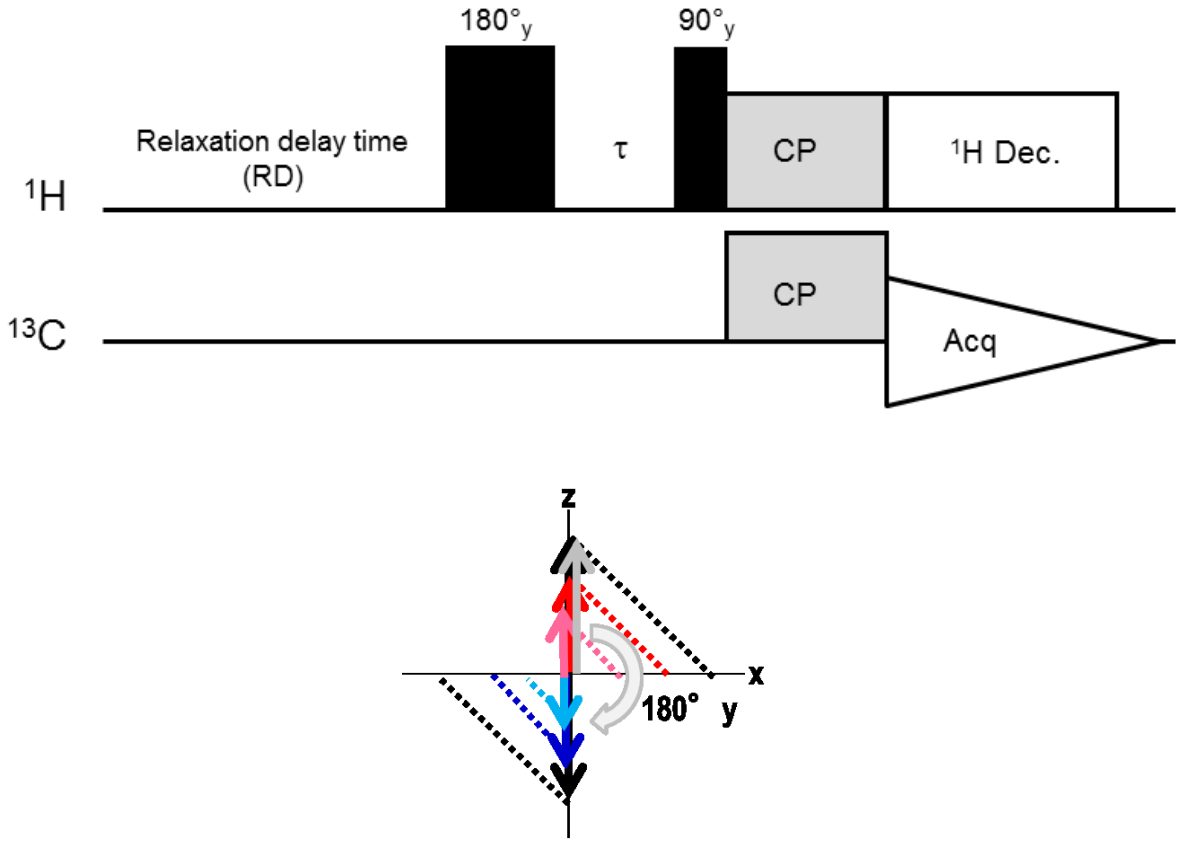

Figure 17. Pulse sequence and vector diagram for the selective ^{13}C signal excitation of components with long or short ^{1}H T_1 in a mixture (RFS method for selective ^{1}H T_1).[18]

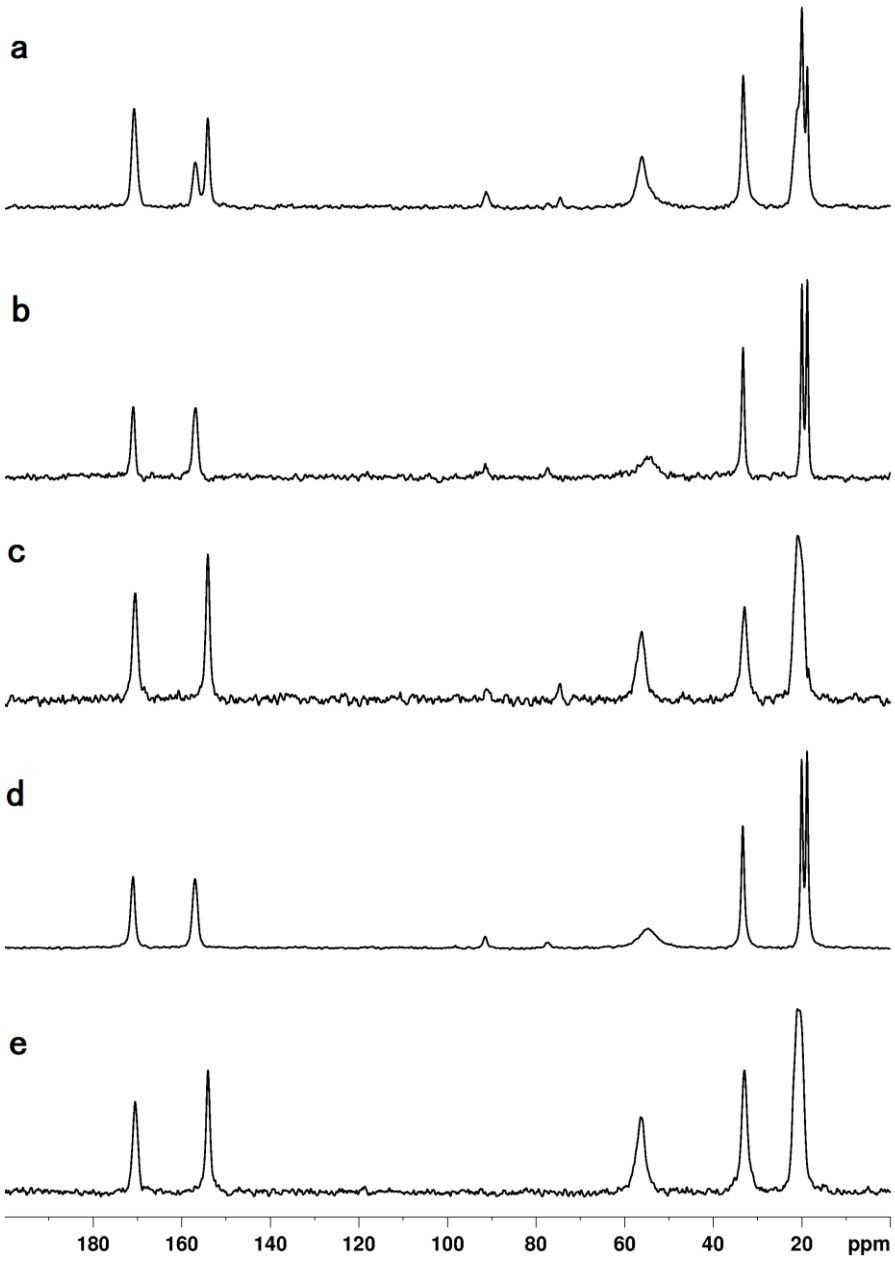

Figure 18. Solid state ^{13}C NMR spectra of bromovalerylurea. (a) Standard ^{13}C CP-MAS spectrum of a 35:65 polymorphic mixture of bromovalerylurea Form I and Form II. (b) Selective ^{13}C signal excitation of bromovalerylurea Form I (RFS method for selective ^{1}H T_1) in a 35:65 polymorphic mixture of bromovalerylurea Form I and Form II. (c) Selective ^{13}C signal excitation of bromovalerylurea Form II (RFS method for selective ^{1}H T_1) in a 35:65 polymorphic mixture of bromovalerylurea Form I and Form II. (d) Standard ^{13}C CP-MAS spectrum of bromovalerylurea Form I. (e) Standard ^{13}C CP-MAS spectrum of bromovalerylurea Form II.

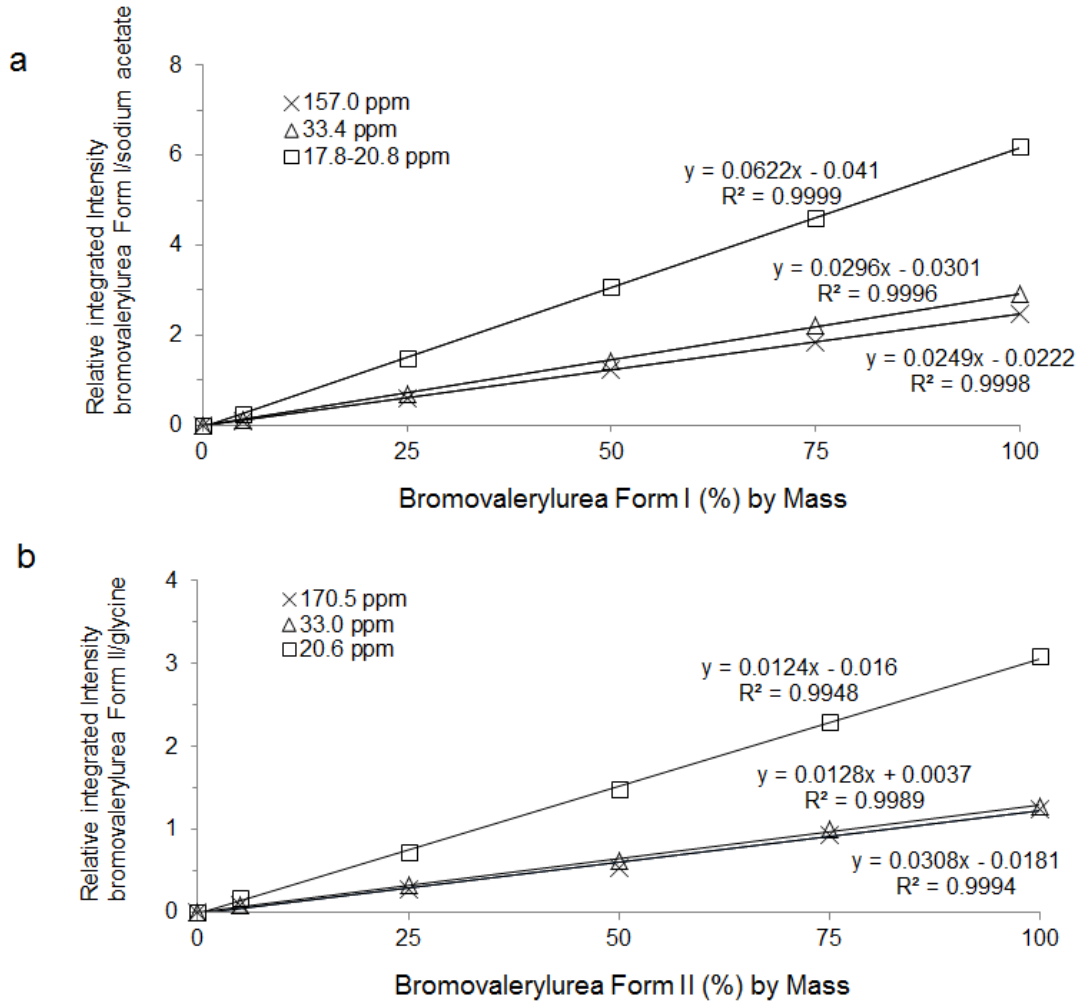

Figure 19. (a) Relative integrated intensity versus quantitation of bromovalerylurea Form I using a physical mixture of bromovalerylurea Form I and sodium acetate (signals at 17.8–20.8, 33.4, and 157.0 ppm for bromovalerylurea Form I calculated against the signal at 26.5 ppm for sodium acetate). (b) Relative integrated intensity versus quantitation of bromovalerylurea Form II using a physical mixture of bromovalerylurea Form II and glycine (signals at 20.6, 33.0 and 170.5 ppm for bromovaleryl urea Form II calculated against the signal at 43.3 ppm for glycine).

Table 6. Results of quantitative analysis of bromovalerylurea Form I (a) and Form II (b) in a 35:65 (w/w) polymorphic mixture of bromovalerylurea Form I and Form II by ^{13}C NMR using the RFS method for selective ^{1}H T_1 with sodium acetate (26.5 ppm) for Form I and glycine (43.3 ppm) for Form II as an internal standard, respectively.

(a)

Quantitated Polymorphs	Quantitation of Form I (%)			Average (%)
	157.0 ppm	33.4 ppm	17.8–20.8 ppm	
Form I	35	35	34	35

(b)

Quantitated Polymorphs	Quantitation of Form II (%)			Average (%)
	170.5 ppm	33.0 ppm	20.6 ppm	
Form II	65	66	66	66

Advanced use of the RFS methods in ^{13}C solid-state NMR spectroscopy

2.4 Selective ^{13}C signal excitation of the component using a combination of several types of RFS method

The pulse sequence in Figure 20, the combination of "RFS method for selective ^{1}H T_1" and "RFS method for long ^{1}H T_{1rho}", was applied to EVE A, which contains 75 mg of ibuprofen, 30 mg of allylisopropylacetylurea, 40 mg of caffeine anhydrous, and 71 mg of excipients. The spectrum of allylisopropylacetylurea was selectively extracted (Figure 21b) from the whole spectrum of EVE A (Figure 21a) at 8 s for τ delay, 150 ms for spin-locking time (τ_{SL}) with low spin-locking power (37.1 kHz) and RD of 20 s with 400 scans, and the same spectrum as the standard ^{13}C CP-MAS spectrum of allylisopropylacetylurea (Figure 21c) was obtained.

In the case of selective signal excitation of ibuprofen from EVE A, the author applied the pulse sequence in Figure 22a, namely the combination of two of "RFS method for selective ^{1}H T_1", which the author termed "RFS method for selective ^{1}H T_1x2". The spectrum of ibuprofen was selectively extracted with the spectrum of cellulose as an excipient with phase inversion (Figure 23b) at 9 s for τ_1 delay, 1 s for τ_2 delay and RD of 20 s with 800 scans. The same spectrum as the standard ^{13}C CP-MAS spectrum of ibuprofen (Figure 23d) was obtained. Furthermore, the spectrum of ibuprofen was clearly extracted (Figure 23c) by applying the pulse sequence in Figure 22b, the combination of "RFS method for selective ^{1}H T_1x2" and "RFS method for long ^{1}H T_{1rho}" at 9 s for τ_1 delay, 1 s for τ_2 delay, 50 ms for τ_{SL} with normal spin-locking power (69.4 kHz) and RD of 20 s with 1600 scans.

A target component in a multicomponent mixture could be extracted in a single experiment by combining more than two types of RFS method (Figure 20 and Figure 22). In the case of EVE A, the ^{13}C signal of caffeine anhydrous was eliminated by setting the appropriate τ delay, at which the proton magnetization showed null using the RFS method for selective ^{1}H T_1 in the first step. In the second step, ^{13}C signals of allylisopropylacetylurea, which had the longest ^{1}H T_{1rho} among the remaining components, were selectively excited using the RFS method for long ^{1}H T_{1rho} (Figure 21b). In contrast, the spectrum of ibuprofen, which had the shortest ^{1}H T_1 among the remaining components, was selectively extracted with the spectrum of cellulose, which had phase inversion, when the RFS method for selective ^{1}H T_1 was applied in the second step as a result of the elimination of allylisopropylacetylurea (Figure 23b). Furthermore, the pure spectrum of ibuprofen was extracted with further addition of the RFS method for long ^{1}H T_{1rho} by elimination of the spectrum of cellulose (Figure 23c). In addition to the four types of basic single RFS method, use of a combination of two or more types of these methods allows greater latitude in the relaxation filtered-selective signal excitation in the mixture.

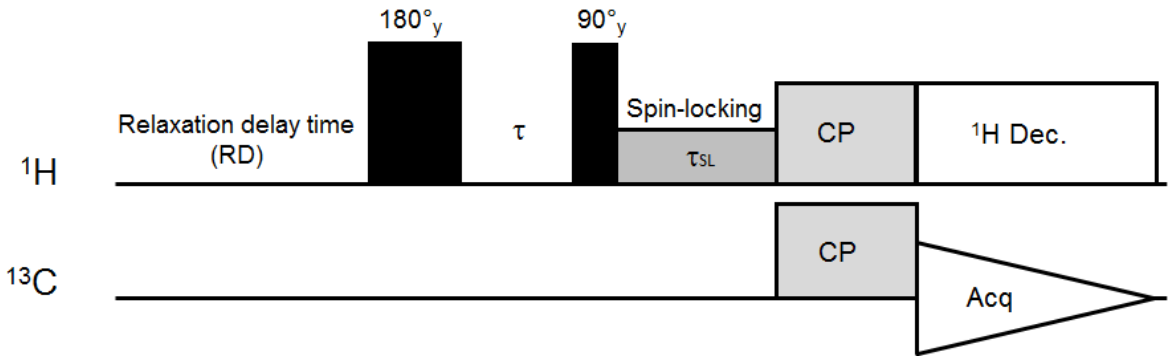

Figure 20. Pulse sequence of the combination of RFS method for selective ^{1}H T_1 and RFS method for long ^{1}H T_{1rho}.

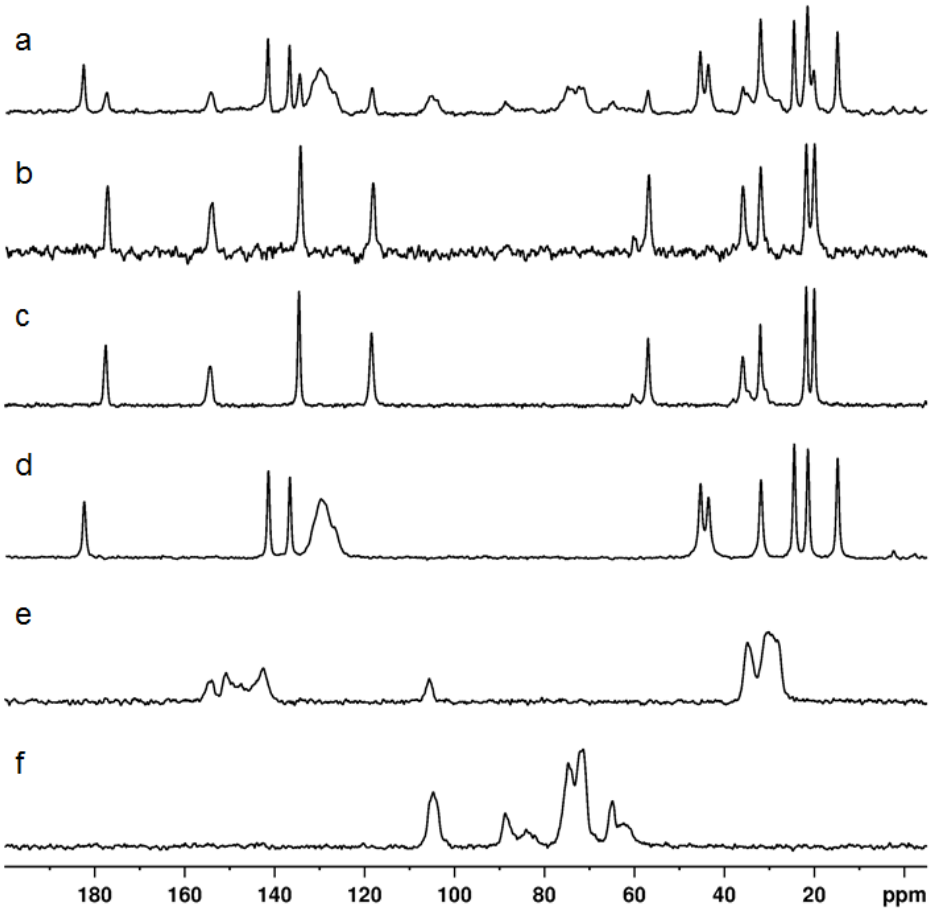

Figure 21. Solid state ^{13}C NMR spectra of EVE A and reference standards. (a) Standard ^{13}C CP-MAS spectrum of EVE A. (b) Selective ^{13}C signal excitation of allylisopropylacetylurea (combination of RFS method for selective ^{1}H T_1 and RFS method for long ^{1}H T_{1rho}) in EVE A. (c) Standard ^{13}C CP-MAS spectrum of allylisopropylacetylurea. (d) Standard ^{13}C CP-MAS spectrum of ibuprofen. (e) Standard ^{13}C CP-MAS spectrum of caffeine anhydrous. (f) Standard ^{13}C CP-MAS spectrum of cellulose.

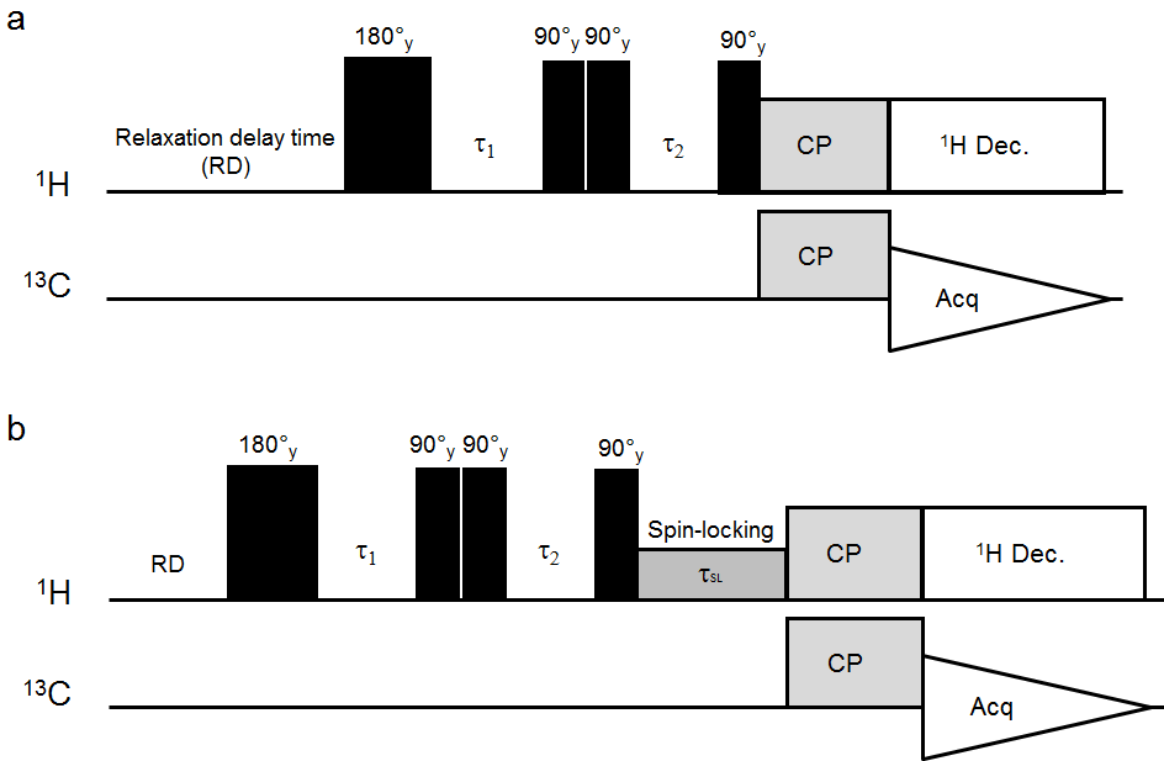

Figure 22. Pulse sequence of the combination of RFS methods (a) Combination of RFS method for selective ^{1}H T_1 and RFS method for selective ^{1}H T_1 (RFS method for selective ^{1}H T_1x2). (b) Combination of RFS method for selective ^{1}H T_1x2 and RFS method for long ^{1}H T_{1rho}.

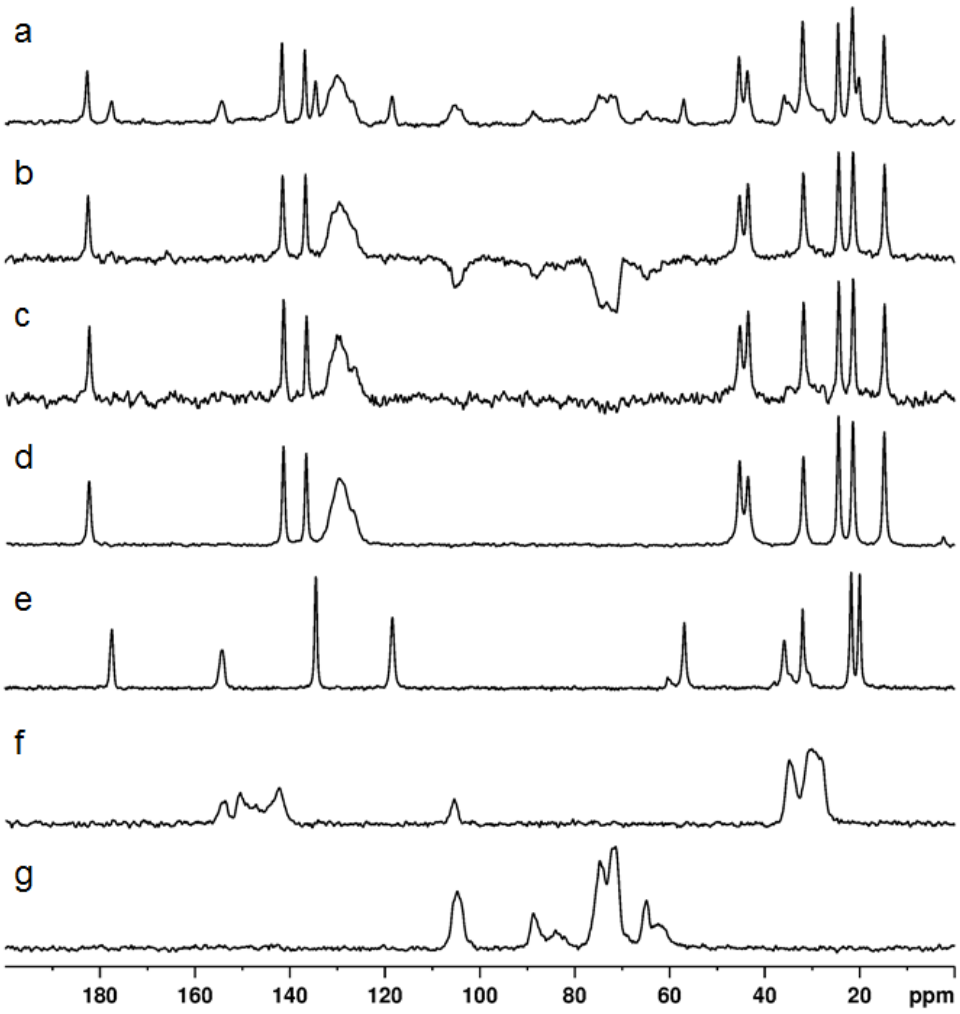

Figure 23. Solid state ^{13}C NMR spectra of EVE A and reference standards. (a) Standard ^{13}C CP-MAS spectrum of EVE A. (b) Selective ^{13}C signal excitation of ibuprofen (RFS method for selective ^{1}H T_1x2) in EVE A. (c) Selective ^{13}C signal excitation of ibuprofen (combination of RFS method for selective ^{1}H T_1x2 and RFS method for long ^{1}H T_{1rho}) in EVE A. (d) Standard ^{13}C CP-MAS spectrum of ibuprofen. (e) Standard ^{13}C CP-MAS spectrum of allylisopropylacetylurea. (f) Standard ^{13}C CP-MAS spectrum of caffeine anhydrous. (g) Standard ^{13}C CP-MAS spectrum of cellulose.

2.5 Application of the flip-back pulse to the RFS methods

The pulse sequence for the selective ^{13}C signal excitation of components with the longest ^{1}H T_{1rho} in the mixture with FB pulse (RFS method for long ^{1}H T_{1rho} with FB) is shown in Figure 24. Crystalline nifedipine was selectively extracted from a physical mixture of 50% crystallinity of nifedipine with 30% PVP K-30 using the RFS method for long ^{1}H T_{1rho} with FB, as shown in Figure 25a (1800 scans, RD = 10 s, τ_{SL} = 150 ms, spin-locking power = 40.6 kHz; 5 h 5 min) and Figure 25b (480 scans, RD = 10 s, τ_{SL} = 150 ms, spin-locking power = 40.6 kHz; 1 h 23 min). A comparison with the spectrum using the RFS method for long ^{1}H T_{1rho} without FB pulse is shown in Figure 25c (360 scans, RD = 50 s, τ_{SL} = 150 ms, spin-locking power = 40.6 kHz; 5 h 1 min).

The sequence consists in adding a ^{1}H 90° pulse, namely an FB pulse after the ^{1}H decoupling scheme. Because RD can be shortened in components with a long ^{1}H T_1 using an FB pulse, efficiency of the relative signal intensity is improved. Because ^{1}H magnetization along the +x axis can be forced to flip back to the +z axis with an FB pulse, the only possible decoupling scheme that can be combined with an FB pulse is a CW decoupling. Further, a multi-pulse decoupling sequence like SPINAL-64[34] or TPPM,[35] which disperses the ^{1}H magnetization all over the transverse plane, cannot be combined with an FB pulse. Although the decoupling efficiency of CW decoupling is inferior to that of multi-pulse decoupling sequences, FB pulse is an attractive way of increasing the relative signal intensity or reducing experimental duration. The author applied the RFS method for long ^{1}H T_{1rho} with FB pulse (Figure 24) to extract the spectrum of crystalline nifedipine from a mixture of crystalline nifedipine and

amorphous solid dispersions of nifedipine with PVP K-30 and successfully extracted the target component with high efficiency (Figure 25).

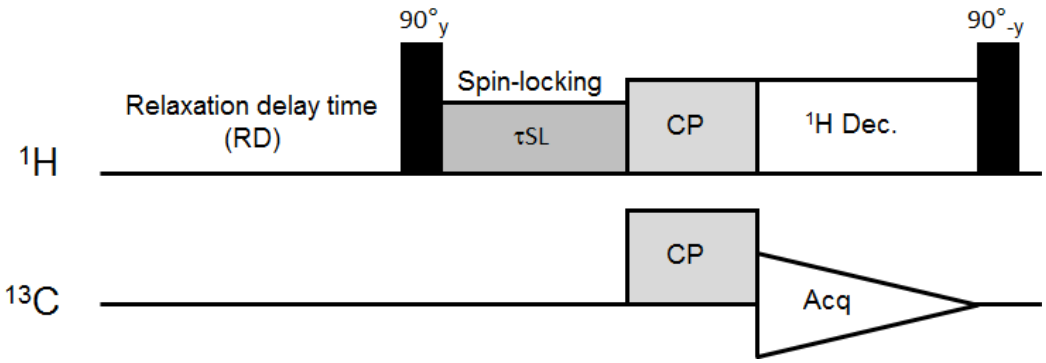

Figure 24. Pulse sequence of RFS method for long ^{1}H T_{1rho} with FB.

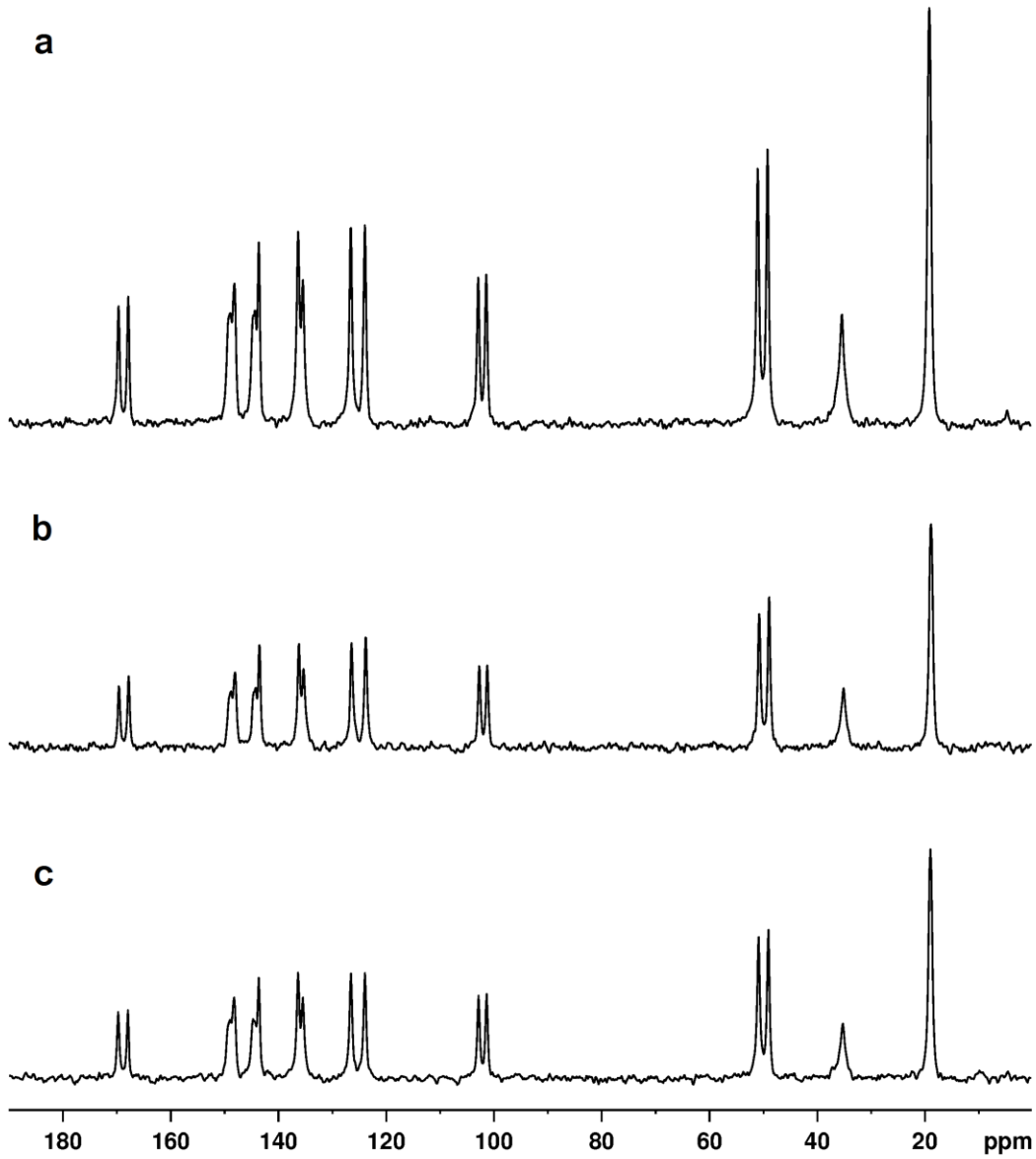

Figure 25. Solid state ^{13}C NMR spectra of crystalline nifedipine in 50% crystallinity of nifedipine with 30% PVP K-30. (a) Selective ^{13}C signal excitation of crystalline nifedipine (RFS method for long ^{1}H T_{1rho} with FB; 1800 scans, RD = 10 s, τ_{SL} = 150 ms, spin-locking power 40.6 kHz; 5 h 5 min). (b) Selective ^{13}C signal excitation of crystalline nifedipine (RFS method for long ^{1}H T_{1rho} with FB; 480 scans, RD = 10 s, τ_{SL} = 150 ms, spin-locking power 40.6 kHz; 1 h 23 min). (c) Selective ^{13}C signal excitation of crystalline nifedipine (RFS method for long ^{1}H T_{1rho} without FB; 360 scans, RD = 50 s, τ_{SL} = 150 ms, spin-locking power 40.6 kHz; 5 h 1 min).

CHAPTER 3

The RFS methods in ^{19}F solid state NMR spectroscopy

3.1 Fluorine-19 CP-MAS NMR spectroscopy of ATC Form I and atorvastatin tablets

Atorvastatin calcium (ATC) (Figure 26) 10 mg drug products were characterized by ^{19}F solid state NMR. The ^{19}F solid state NMR spectra of the atorvastatin tablets were compared to those of ATC Form I references acquired in the same ^{19}F CP-MAS experiment to identify polymorph(s) present. The ^{19}F CP-MAS NMR spectra of Atorvastatin 10 mg [NP] and Atorvastatin 10 mg "Nichiiko" were closely similar with a mixture of a trace amount of ATC Form I included in a disordered solid form, primarily as amorphous form (Figure 27a and Figure 27b). Further, proton spin-lattice relaxation time (^1H T_1 = 3.0 s for Atorvastatin 10 mg [NP] and 3.5 s for Atorvastatin 10 mg "Nichiiko"), proton spin-lattice relaxation time in the rotating frame (^1H T_{1rho} = 13.5 ms for Atorvastatin 10 mg [NP] and 16.6 ms for Atorvastatin 10 mg "Nichiiko") of API, composition of API and additives, description, appearance, tablet size, and weight (approx. 88 mg) were also closely similar between Atorvastatin 10 mg [NP] and Atorvastatin 10 mg "Nichiiko," and these two product formulations can accordingly be considered as equivalent for investigation. In contrast, Lipitor® 10 mg Tablets were consistent with ATC Form I (Figure 27c and Figure 27d) as an

API. Fluorine resonances in the Atorvastatin 10 mg [NP] and Atorvastatin 10 mg "Nichiiko" spectra were broader than the ATC Form I reference spectra but the chemical shifts were closely consistent with ATC Form I.

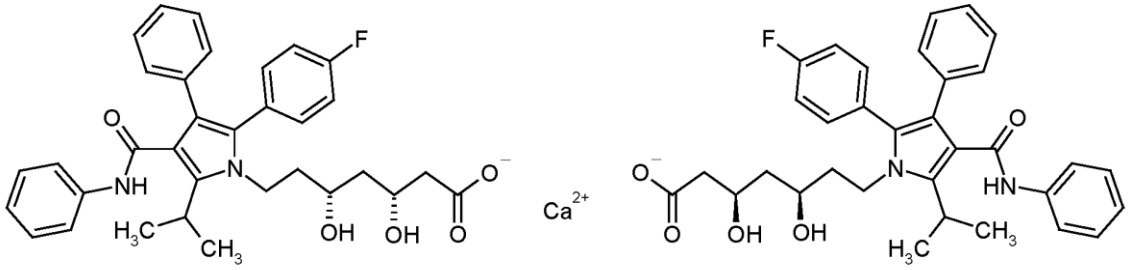

Figure 26. Chemical structure of atorvastatin calcium.

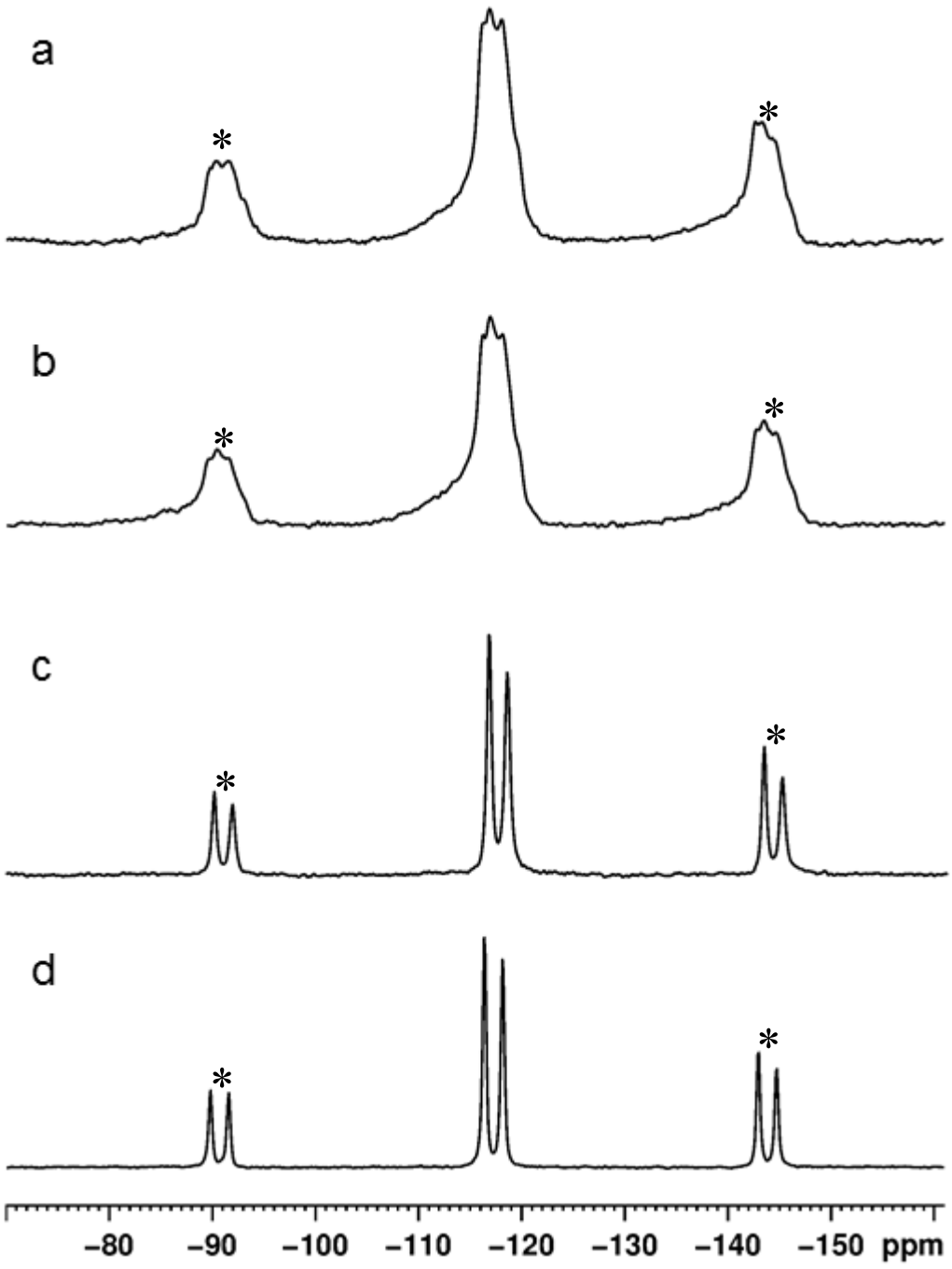

Figure 27. Solid state ^{19}F CP-MAS NMR spectra. (a) Atorvastatin 10 mg [NP], (b) Atorvastatin 10 mg "Nichiiko," (c) Lipitor® 10 mg tablets, (d) ATC Form I. *Spinning side bands.

3.2 The RFS methods for ^{19}F solid state NMR spectroscopy

The author initially applied the RFS methods for ^{19}F CP-MAS experiments which utilize the difference in ^{1}H T_{1rho} or ^{1}H T_1 of each component, and used these to selectively extract the targeted component having ^{19}F atoms in their structure from a mixture of several components (Figure 28). Further, the author developed new RFS methods for DD-MAS experiments which utilize the difference in X T_{1rho} or X T_1 of each component, and used these to selectively extract the targeted component in the isotope-labeled compound (e.g. labeled by ^{13}C or ^{15}N) or a naturally highly abundant element such as fluorine-19 or phosphorus-31 (Figure 29). The RFS methods termed "RFS method for long ^{1}H T_{1rho}" and "RFS method for long X T_{1rho}" selectively excite the component with the longest ^{1}H T_{1rho} or longest X T_{1rho} in a mixture. In contrast, the RFS methods termed "RFS method for selective ^{1}H T_{1rho}" and "RFS method for selective X T_{1rho}" selectively excite the components with "long or short ^{1}H T_{1rho}" or "long or short X T_{1rho}" in a mixture. Similarly, the RFS methods termed "RFS method for long ^{1}H T_1" and "RFS method for long X T_1" selectively excite the component with the longest ^{1}H T_1 or longest X T_1 in a mixture, and the RFS method termed "RFS method for selective ^{1}H T_1" and "RFS method for selective X T_1" selectively excite the components with "long or short ^{1}H T_1" or "long or short X T_1" in a mixture.

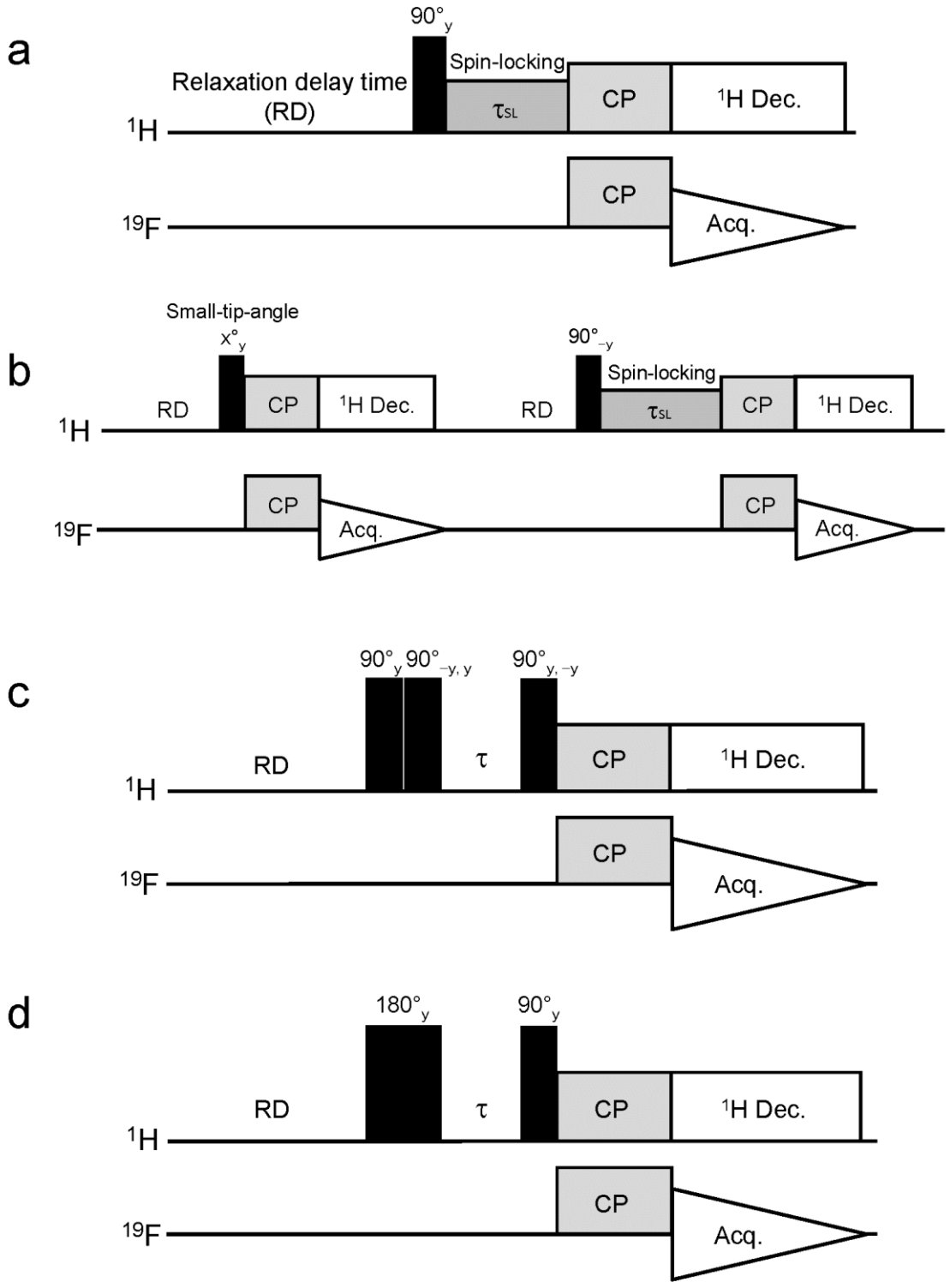

Figure 28. Pulse sequences for RFS methods for ^{19}F CP-MAS experiments using the difference in ^{1}H T_{1rho} or ^{1}H T_1. (a) RFS method for long ^{1}H T_{1rho}. (b) RFS method for selective ^{1}H T_{1rho}. (c) RFS method for long ^{1}H T_1. (d) RFS method for selective ^{1}H T_1.

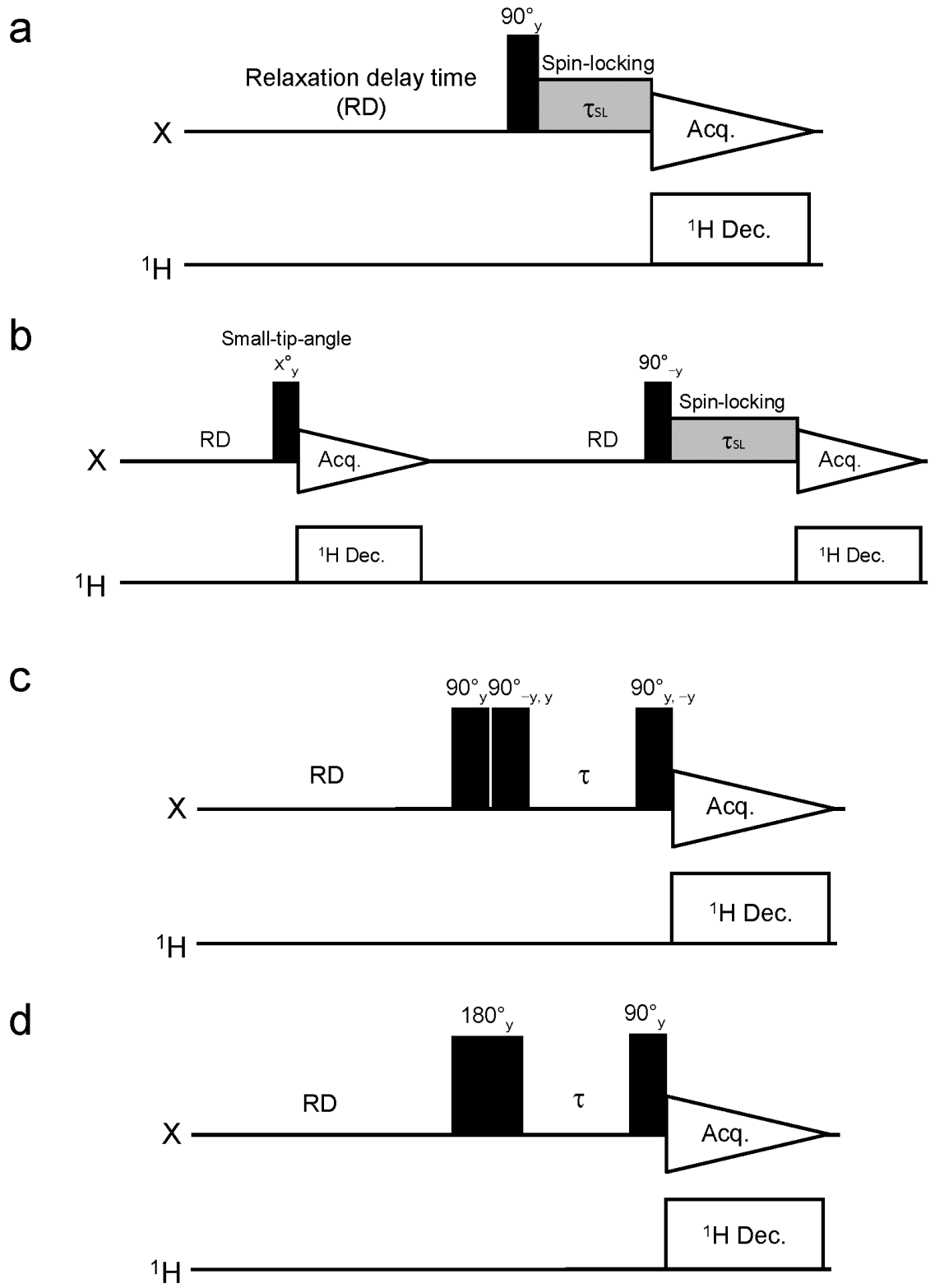

Figure 29. Pulse sequences for RFS methods for X DD-MAS experiments using the difference in X T_{1rho} or X T_1. (a) RFS method for long X T_{1rho}. (b) RFS method for selective X T_{1rho}. (c) RFS method for long X T_1. (d) RFS method for selective X T_1.

3.3 Selective ^{19}F signal excitation of the target component (amorphous form of ATC) in a mixture using the RFS method

The author applied the RFS method to the selective ^{19}F signal excitation of the target component from the atorvastatin tablets supplied by generic drug suppliers. For this purpose, the author selected the RFS method for selective ^{1}H T_1 because of its shorter experimental duration, based on the shorter relaxation time of ^{1}H T_1 than ^{19}F T_1. Further, the relaxation times of ^{19}F T_1 in ATC Form I and the amorphous form of ATC in the Atorvastatin 10 mg [NP] and Atorvastatin 10 mg "Nichiiko" are similar (7.2 s and 8.0 s for the two signals in ATC Form I vs. 10.3 s for the amorphous form of ATC, a difference of only 1.3 times), while ^{1}H T_{1rho} are 16.6 m for the amorphous form of ATC and 16.7 m for crystalline ATC Form I, and ^{19}F T_{1rho} values are both >1000 ms for the amorphous form of ATC and for crystalline ATC Form I (Table 7). Although the RFS method for long ^{1}H T_1 (Figure 28c) might also be thought suitable for the selective ^{19}F signal excitation of ATC Form I, this was prevented by the small difference in ^{1}H T_1 (5.0 s for ATC Form I and 3.0 s for the amorphous form of ATC, a difference of only 1.7 times). However, given the success of ^{19}F signal excitation of the target component using the RFS method for selective ^{1}H T_1 (Figure 28d), despite the difference in ^{1}H T_1, the RFS method for selective ^{1}H T_1 was considered to provide better discrimination of components than the RFS method for long ^{1}H T_1. These results mean that the RFS method for long ^{1}H T_1 is unable to discriminate components which have a small difference in ^{1}H T_1. When the signals of vanished component(s)

were null for the τ delay, the signal intensity of the extracted target component became quite small, and did not have sufficient signal intensity for detection by the small difference in ^{1}H T_1. This is because this method uses τ delay, whose signal intensity gradually decreases to null. In contrast, the RFS method for selective ^{1}H T_1 can discriminate different components having small differences in ^{1}H T_1 because it uses the unique τ delay as a null point for vanished components and has sufficient signal intensity for detection of the extracted target component.

For selective ^{19}F signal excitation of the amorphous form of ATC using the RFS method for selective ^{1}H T_1, a preliminary measurement was performed to optimize the length of τ delay in the pulse sequence of Figure 28d. This was done by plotting the correlation between the τ delay and signal intensity, using the pulse sequence of the inversion recovery (180°–τ–90°) on proton magnetization before the CP step in the 2D NMR experiment.[33] Optimizing the τ delay for selective excitation of the amorphous form of ATC required only 25 min. Figure 30a shows the correlation between τ delay and signal intensity using the pulse sequence of Figure 28d for ATC Form I with a RD of 7.0 s. Null point was optimized as 2.50 s from the inversion recovery (180°–τ–90°) pulse sequence, whose value also set for τ delay (τ) in the pulse sequence of Figure 28d, and successfully detected ^{19}F signals of the amorphous form of ATC only from Atorvastatin 10 mg [NP], which included a trace amount of ATC Form I with amorphous form of ATC (1600 scans, RD = 7.0 s, τ = 2.50 s; experimental duration of 2 h 51 min) (Figure 31b).

Table 7. Relaxation time values of ^{1}H T_1, ^{1}H T_{1rho}, ^{19}F T_1 and ^{19}F T_{1rho} for amorphous form of ATC in Atorvastatin 10 mg "Nichiko" and ATC Form I

Polymorphism	^{1}H T_1 (s)	^{1}H T_{1rho} (msec)	^{19}F T_1 (s)	^{19}F T_{1rho} (msec)
Amorphous form of ATC in Atorvastatin 10 mg "Nichiiko"	3.0	16.6	10.3 (-117 ppm)	>1000 (-117 ppm)
ATC Form I	5.0	16.7	7.2 (-116 ppm)	>1000 (-116 ppm)
			8.0 (-118 ppm)	>1000 (-118 ppm)

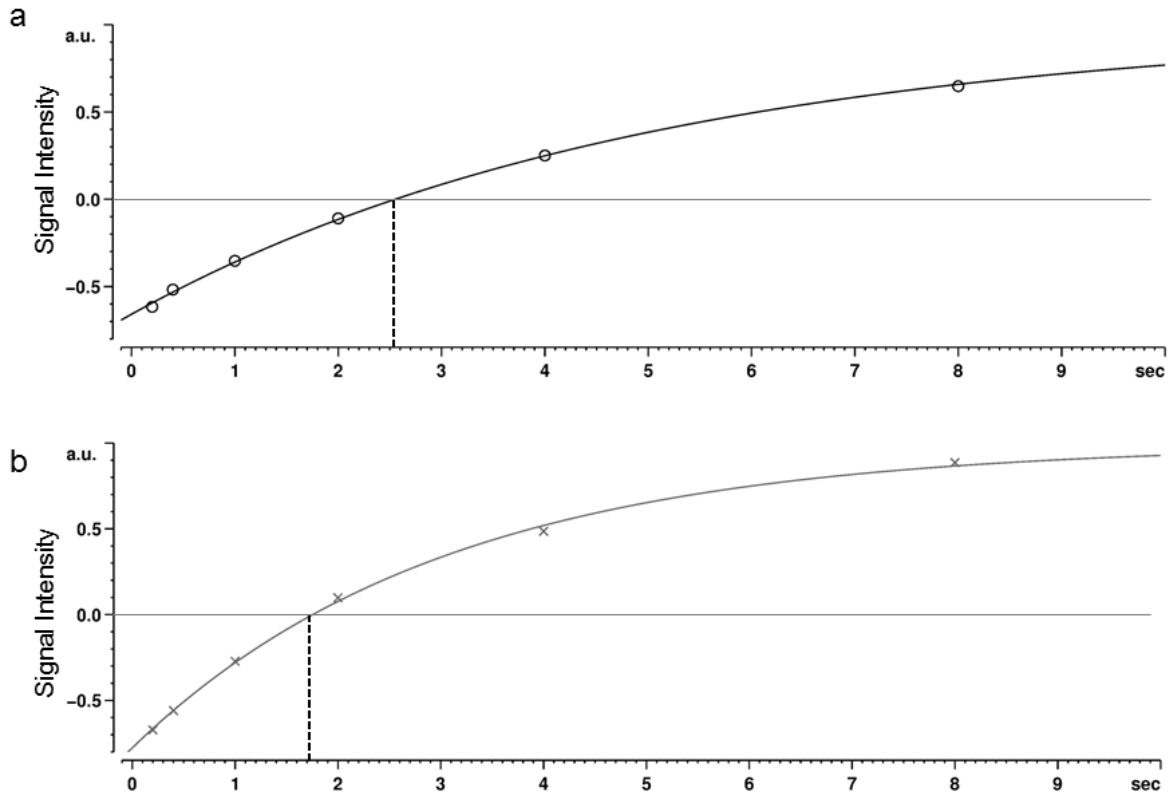

Figure 30. Correlation between τ delay and signal intensity using the RFS method for selective ^{1}H T_1 for ATC. (a) ATC Form I. (b) Atorvastatin 10 mg [NP].

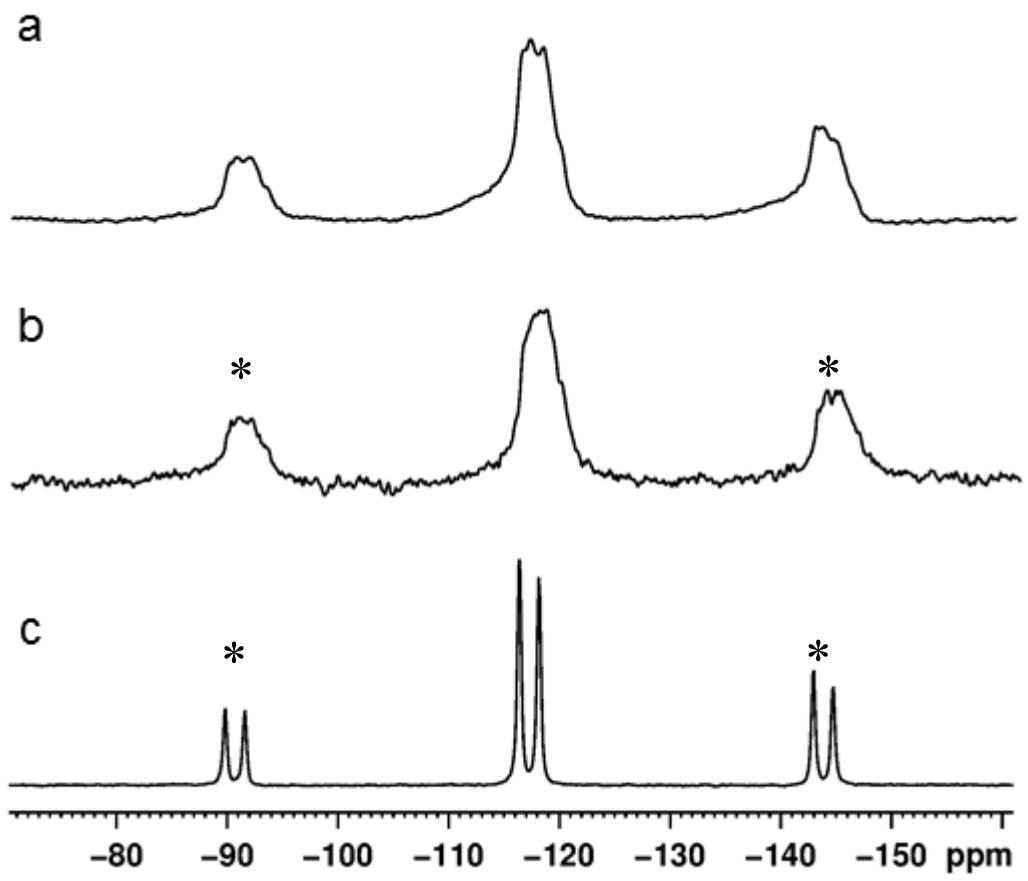

Figure 31. Solid state ^{19}F NMR spectra of ATC. (a) Standard ^{19}F CP-MAS spectrum of Atorvastatin 10 mg [NP]. (b) Selective ^{19}F signal excitation of amorphous form of ATC (RFS method for selective ^{1}H T_1) in Atorvastatin 10 mg [NP]. (c) Standard ^{19}F CP-MAS spectrum of ATC Form I. *Spinning side bands.

3.4 Selective ^{19}F signal excitation of the target component (ATC Form I) and detection limits in a mixture using the RFS method

For selective ^{19}F signal excitation of the ATC Form I in a mixture using the RFS method for selective ^{1}H T_1, the author set 7.0 s for RD and 1.72 s for τ delay in the pulse sequence of Figure 28d. These values were optimized using the pulse sequence of the inversion recovery (180°–τ–90°) on proton magnetization before the CP step in the 2D NMR experiment (Figure 30b) in the pulse sequence of Figure 28d.

To examine the detection and qualification limits of selective ^{19}F signal excitation using the RFS method, the author analyzed two physical mixtures of ATC Form I and pulverized Atorvastatin 10 mg "Nichiiko" [ratios: 0.05 (5% w/w) and 0.005 (0.5% w/w) of ATC Form I to 1.0 of Atorvastatin 10 mg tablets "Nichiiko" by weight)] using the RFS method for selective ^{1}H T_1.

Although the author was able to confirm the existence of ATC Form I in the physical mixture of 5% w/w of ATC Form I addition into Atorvastatin 10 mg "Nichiiko" using the standard ^{19}F CP-MAS experiment (256 scans, RD = 7.0 s), confirmation for the physical mixture of 0.5% w/w of ATC Form I addition into Atorvastatin 10 mg "Nichiiko" (256 scans, RD = 7.0 s) was slightly difficult (Figure 32a and Figure 32c). In contrast, ^{19}F signals of ATC Form I was clearly detectable in the physical mixture of 0.5% w/w of ATC Form I addition into Atorvastatin 10 mg "Nichiiko" using the RFS method for selective ^{1}H T_1 (6400 scans, RD = 7.0 s, τ = 1.72 s; experimental duration of 15 h 34 min), with sufficient

signal-to-noise ratio (S/N = 10.3) for qualification (Figure 32d). Further, the author could detect a trace amount of ATC Form I in Atorvastatin 10 mg "Nichiiko" (8192 scans, RD = 7.0 s, τ = 1.72 s; experimental duration of 19 h 56 min), which was estimated to be less than the 0.5% w/w level compared with the 0.5% w/w of ATC Form I addition into Atorvastatin 10 mg "Nichiiko," as based on a composition of signal intensities in CP-MAS experiments (Figure 32c and Figure 33a) and the signal-to-noise ratios of the RFS method for selective ^{1}H T_1 experiments (Figure 32d and Figure 33b). In this case, even though the difference in relaxation time was very small, the author succeeded in the detection of less than the 0.5% w/w level of the targeted component without any other components. If the difference in relaxation time were large, the detection limit would be lower.

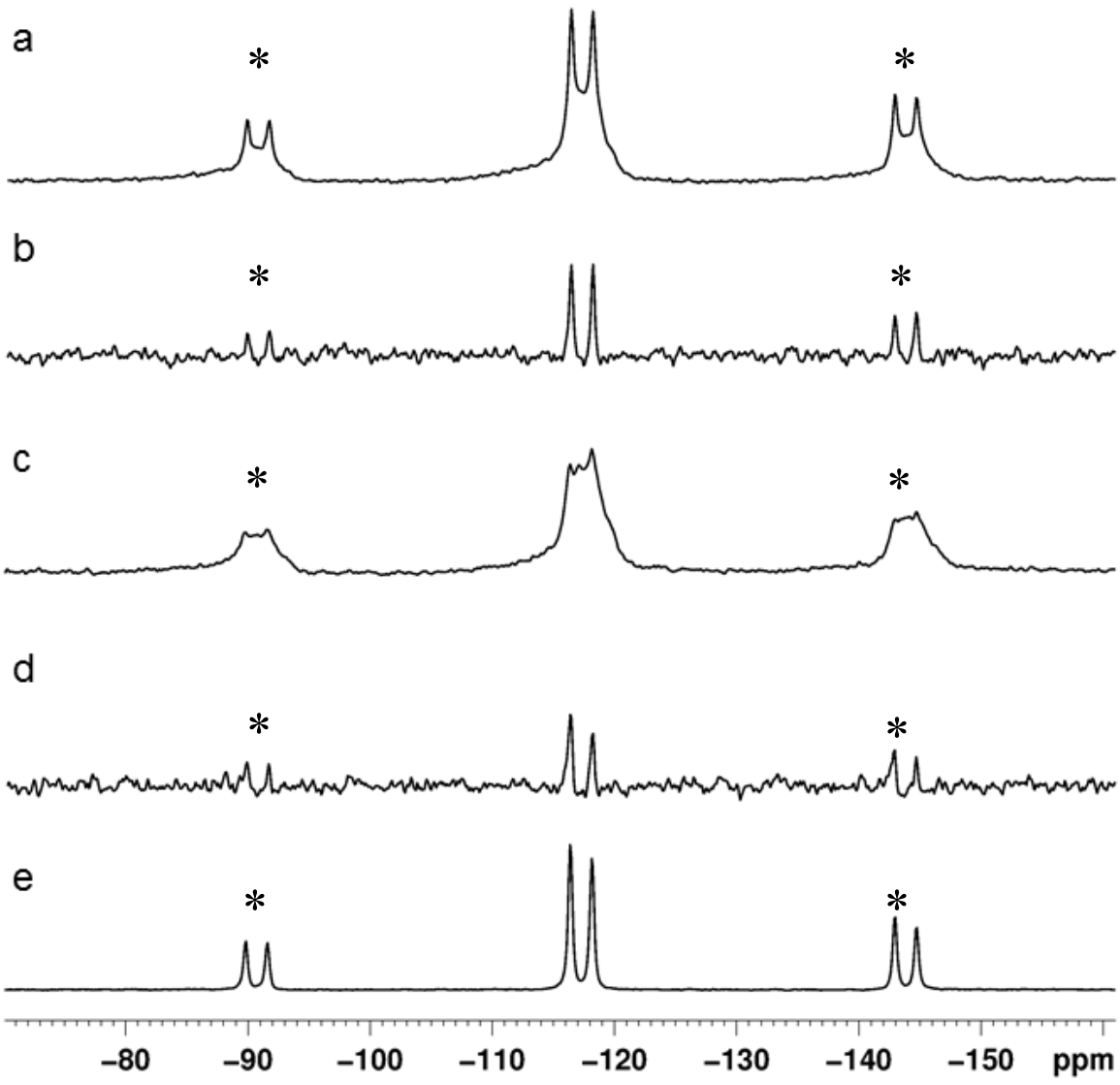

Figure 32. Solid state ^{19}F NMR spectra of ATC. (a) Standard ^{19}F CP-MAS spectrum of a physical mixture of 5% w/w of ATC Form I in Atorvastatin 10 mg "Nichiiko." (b) Selective ^{19}F signal excitation of ATC Form I (RFS method for selective ^{1}H T_1) in a physical mixture of 5% w/w of ATC Form I in Atorvastatin 10 mg "Nichiiko." (c) Standard ^{19}F CP-MAS spectrum of a physical mixture of 0.5% w/w of ATC Form I in Atorvastatin 10 mg "Nichiiko." (d) Selective ^{19}F signal excitation of ATC Form I (RFS method for selective ^{1}H T_1) in a physical mixture of 0.5% w/w of ATC Form I in Atorvastatin 10 mg "Nichiiko." (e) Standard ^{19}F CP-MAS spectrum of ATC Form I. *Spinning side bands.

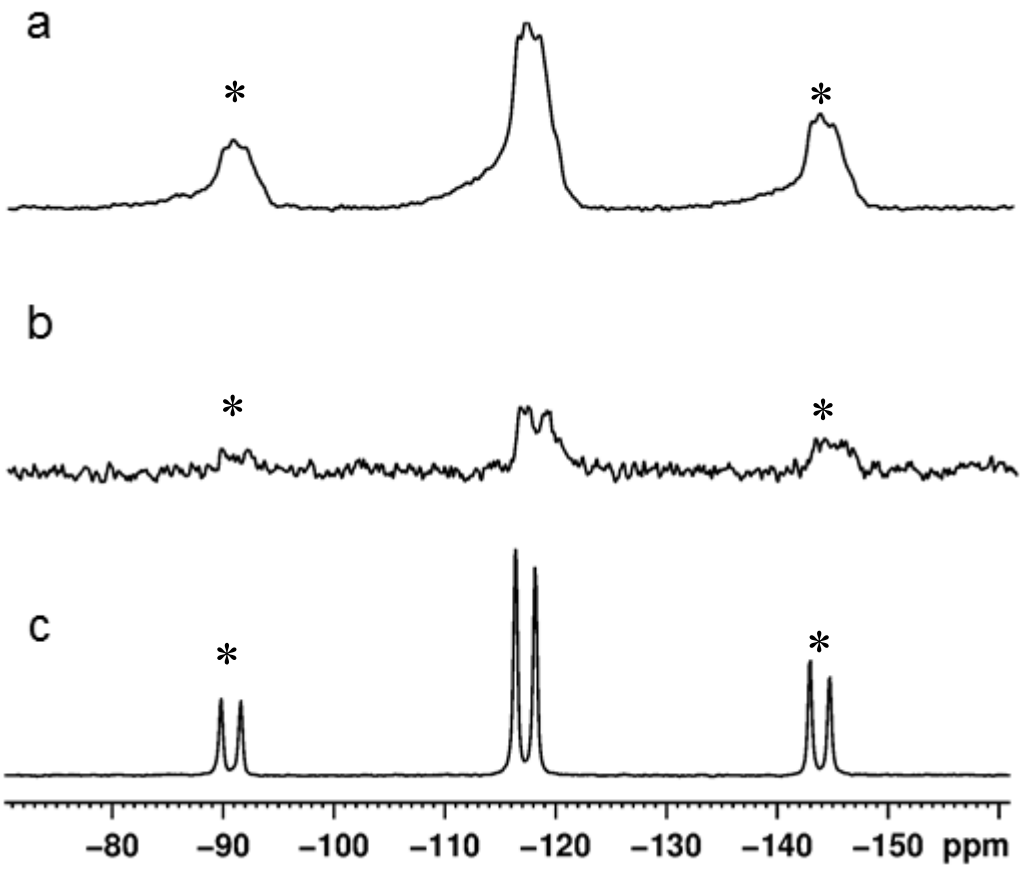

Figure 33. Solid state ^{19}F NMR spectra of ATC. (a) Standard ^{19}F CP-MAS spectrum of Atorvastatin 10 mg "Nichiiko." (b) Selective ^{19}F signal excitation of ATC Form I (RFS method for selective ^{1}H T_1) in Atorvastatin 10 mg "Nichiiko." (c) Standard ^{19}F CP-MAS spectrum of ATC Form I. *Spinning side bands.

EXPERIMENTAL SECTION

Materials

The RFS methods for ^{1}H T_{1rho} in ^{13}C solid state NMR spectroscopy

The commercially available analgesic and antipyretic Saridon® Ace was purchased from Daiichi Sankyo Co., Ltd. (Tokyo, Japan) and milled before sample packing. Ethenzamide was supplied by Iwaki Seiyaku Co., Ltd. (Tokyo, Japan), and acetaminophen by MP Biomedicals LLC (Irvine, CA, USA). Glycine and bromovaleryl urea were obtained from Tokyo Chemical Industry Ltd. (Tokyo, Japan). Alpha-lactose monohydrate was purchased from Kanto Chemical Co., Inc. (Tokyo, Japan) and β-cyclodextrin (β-CD) from Sigma-Aldrich (St. Louis, MO, USA), and equal amounts of both were weighed out and finely milled together as the test mixture. Indomethacin γ form, nifedipine and PVP K-30 were purchased from Wako Chemicals (Osaka, Japan). All materials were used without further purification. Indomethacin α form was crystallized from ethanol-water at 80 °C.[36]

Five physical mixtures of nifedipine and acetaminophen (ratios: 0.1, 0.5, 1.0, 1.5, and 2.0 of nifedipine to 1.0 of acetaminophen as an internal standard by weight) were prepared using a vortex mixer with 3-min mixing. Each of the mixtures corresponded to 5%, 25%, 50%, 75%, and 100% crystallinity for the standard curve. For samples for use in quantitative analysis of crystallinity, amorphous solid dispersions of nifedipine with PVP K-30 as the polymeric carriers were prepared in three mixing ratios (35:30, 40:20, and 42.5:15 by weight) by a melt-quenching method, followed by trituration and sieving (#60 mesh). These three mixtures were then mixed with crystalline

nifedipine and acetaminophen as physical mixtures of 50% crystalline nifedipine with different ratios (30%, 20%, and 15%) of PVP K-30 using a vortex mixer for 3 min.

Five physical mixtures of indomethacin α form and glycine (ratios: 0.25, 1.25, 2.5, 3.75and 5.0 to 1.0 of glycine as an internal standard by weight) were prepared using a vortex mixer with 3-min mixing. The mixtures corresponded to 5%, 25%, 50%, 75%, and 100%, respectively, of indomethacin α form in a polymorphic mixture for the standard curve. A 50:50 polymorphic mixture of indomethacin α form and γ form was prepared and then mixed with glycine using a vortex mixer for 3 min.

The RFS methods for ^{1}H T_1 in ^{13}C solid state NMR spectroscopy

The commercially available products Saridon® Ace was purchased from Daiichi Sankyo Co., Ltd. (Tokyo, Japan) and EVE A was purchased from SS Pharmaceutical Co., Ltd. (Tokyo, Japan), and were milled before sample packing. Ethenzamide was supplied by Iwaki Seiyaku Co., Ltd. (Tokyo, Japan), and acetaminophen by MP Biomedicals LLC (Irvine, CA, USA). Glycine and bromovalerylurea were obtained from Tokyo Chemical Industry Ltd. (Tokyo, Japan). Sodium acetate and α-lactose monohydrate were purchased from Kanto Chemical Co., Inc. (Tokyo, Japan) and allylisopropylacetylurea was purchased from Sigma-Aldrich (Saint Louis, MO, USA). Caffeine anhydrous, ibuprofen, nifedipine and PVP K-30 were purchased from Wako Chemicals (Osaka, Japan). All materials were used without further purification.

Amorphous lactose was prepared by freeze drying an aqueous 10% w/v lactose solution using a freeze dryer (Virtis genesis 25EL; SP Scientific, Stone Ridge, NY, USA). Bromovalerylurea Form I was prepared by dissolving bulk powder in methanol at 65 °C, then cooling in an ice bath.[37] Bromovalerylurea Form II was obtained by

heating Form I at 130 °C for 1.5 h.[38] Crystalline allylisopropylacetylurea was obtained by recrystallization from MeOH-H_2O (10:1) at 40 °C then cooling in an ice bath before use.

Five physical mixtures of nifedipine and acetaminophen (ratios: 0.1, 0.5, 1.0, 1.5, and 2.0 of nifedipine to 1.0 of acetaminophen as an internal standard by weight) were prepared using a vortex mixer with 3-min mixing. These mixtures corresponded to 5%, 25%, 50%, 75% and 100% crystallinity for the standard curve, respectively. Amorphous solid dispersions of nifedipine with PVP K-30 as the polymeric carriers were prepared by a melt-quenching method. Samples of physical mixtures of 50% crystallinity of nifedipine with different ratios (30%, 20%, and 15% by w/w) of PVP K-30 were prepared by mixing crystalline nifedipine and amorphous solid dispersions of nifedipine with PVP K-30 using a vortex mixer for 3 min. For samples for quantitative analysis of crystallinity, these mixtures were then mixed with acetaminophen using a vortex mixer for 3 min. A sample of 5% crystallinity of nifedipine with 30% of PVP K-30 was prepared by mixing crystalline nifedipine and amorphous solid dispersions of nifedipine with PVP K-30 using a vortex mixer with 3-min mixing.

Four physical mixtures of α-lactose monohydrate and acetaminophen (ratios: 0.5, 1.0, 1.5, and 2.0 of α-lactose monohydrate to 1.0 of acetaminophen as an internal standard by weight) were prepared using a vortex mixer with 3-min mixing. The mixtures corresponded to 25%, 50%, 75%, and 100% crystallinity, respectively, for the standard curve. For samples for quantitative analysis of crystallinity, mixtures of α-lactose monohydrate and amorphous lactose were prepared in three mixing ratios (25:75, 50:50, and 75:25 by weight), then mixed with acetaminophen using a vortex mixer for 3 min.

Five physical mixtures of bromovalerylurea Form I and sodium acetate (ratios: 1.0, 5.0, 10.0, 15.0 and 20.0 of bromovalerylurea Form I to 1.0 of sodium acetate as an internal standard by weight) were prepared using a vortex mixer with 3-min mixing. The mixtures corresponded to 5%, 25%, 50%, 75%, and 100%, respectively, of bromovalerylurea Form I in a polymorphic mixture for the standard curve.

Five physical mixtures of bromovalerylurea Form II and glycine (ratios: 0.25, 1.25, 2.5, 3.75 and 5.0 of bromovalerylurea Form II to 1.0 of glycine as an internal standard by weight) were prepared using a vortex mixer with 3-min mixing. The mixtures corresponded to 5%, 25%, 50%, 75%, and 100%, respectively, of bromovalerylurea Form II in a polymorphic mixture for the standard curve. A 35:65 polymorphic mixture of bromovalerylurea Form I and Form II was prepared and then mixed with sodium acetate or glycine using a vortex mixer for 3 min.

All samples were triturated and sieved (#60 mesh) before mixing.

The RFS methods for ^{1}H T_{1rho}, X T_{1rho}, ^{1}H T_1 and X T_1 in ^{19}F solid state NMR spectroscopy

Atorvastatin calcium (ATC) Form I and commercial Lipitor® 10 mg Tablets were obtained in-house at Astellas Pharm Inc. (Tokyo, Japan). Atorvastatin 10 mg [NP] was purchased from Nipro Pharma Corporation (Osaka, Japan), and Atorvastatin 10 mg "Nichiiko" was purchased from Nichi-iko Pharmaceuticals Co., Ltd. (Toyama, Japan). All tablets were pulverized and all materials were used without further purification.

Two physical mixtures of ATC Form I and pulverized Atorvastatin 10 mg "Nichiiko" [ratios: 0.05 (5% w/w) and 0.005 (0.5% w/w) to 1.0 of Atorvastatin 10 mg

"Nichiiko" by weight) were prepared by mixing on a vortex mixer for 3 min. The batch sizes were that 5.0 mg of ATC Form I was added to the 88 mg of pulverized ATC tablets for 5% ATC Form I additional sample, and 1.0 mg of ATC Form I was added to the 176 mg of pulverized ATC tablets for 0.5% ATC Form I additional sample.

Solid state NMR spectroscopy

The RFS methods for ^{1}H T_{1rho} and ^{1}H T_1 in ^{13}C solid state NMR spectroscopy

All ^{13}C solid state NMR spectra were recorded using an AVANCE III 400WB NMR spectrometer (Bruker Biospin K. K., Kanagawa, Japan). Powder samples were placed into 4-mm zirconia rotors. All spectra were acquired using ramp.100 (linear ramp on ^{1}H channel with 100% to 50% amplitude) for variable-amplitude cross-polarization (VACP) and continuous wave (CW) decoupling (in FB pulse experiments) or SPINAL-64 (in all other experiments) for high-power proton decoupling. Magic angle spinning (MAS) was applied at a rotational speed of 14 kHz. The relaxation delay time (RD) for each of the RFS experiments was set at 1.2 to 1.4 times the ^{1}H T_1 of the targeted component to ensure efficiency. The total scan time for each sample depended on the required signal-to-noise ratio. Pertinent acquisition parameters included a CP contact time of 1.75 ms and a ^{1}H 90° pulse of 3.6 μs (corresponding to nutation frequency of 69.4 kHz). The chemical shifts of ^{13}C signals were referenced to TMS at 0 ppm with sample substitution referencing the carbonyl signal in external glycine (δ = 176.03 ppm). A total of 2048 data points were acquired for each experiment. All data were collected at ambient probe temperature.

The RFS methods for ^{1}H T_{1rho}, X T_{1rho}, ^{1}H T_1 and X T_1 in ^{19}F solid state NMR spectroscopy

All ^{19}F solid state NMR spectra were recorded using an AVANCE III HD 600 NMR spectrometer (Bruker Biospin K. K., Kanagawa, Japan). Powder samples were placed into 2.5-mm zirconia rotors. All spectra were acquired using ramp.100 (linear ramp on ^{1}H channel with 100% to 50% amplitude) for variable-amplitude cross-polarization (VACP) and SPINAL-64 for high-power proton decoupling. Magic angle spinning (MAS) was applied at a rotational speed of 15 kHz. To ensure efficiency, relaxation delay time (RD) for each of the RFS experiments was set at 1.2 to 1.4 times the ^{1}H T_1 for ^{19}F CP-MAS or the ^{19}F T_1 for DD-MAS experiments of the targeted component. The total scan time for each sample depended on the required signal-to-noise ratio. Pertinent acquisition parameters included a CP contact time of 2.00 ms and a ^{1}H 90° pulse of 2.5 μs (corresponding to a nutation frequency of 100 kHz). The spectra were referenced using an external sample of trifluoroacetic acid, with resonance set to -76.54 ppm.

SUMMARY AND CONCLUSIONS

Solid state NMR is a specific, non-destructive analytical method which clarifies the structure of a material as well as that of any other contaminants present. The author has focused on the development of new analytical methods and their application in solid mixtures using relaxation filter-selective signal excitation (RFS) methods in ^{13}C solid state NMR and ^{19}F solid state NMR. The RFS methods in^{13}C solid state NMR have been successfully used to selectively excite ^{13}C signals of the target component in mixtures and provide an accurate estimation of the quantitative value of the target component over the wide range of 5% to 100%. Furthermore, combination of two or more of these methods expanded the selectivity of signal excitation for the target component from the multicomponent mixture, and application of FB pulse further enhanced their practicality. Also, the RFS methods can be applied to CP-MAS, DD-MAS and SP-MAS in ^{19}F solid state NMR using the difference in ^{1}H T_{1rho}, ^{1}H T_1, X T_{1rho} or X T_1. Regarding the detection of trace amounts of contaminated components, the author successfully used the RFS method for selective ^{1}H T_1 in ^{19}F solid state NMR in selective signal excitation of less than 0.5% w/w of a crystalline component (ATC Form I) in atorvastatin 10 mg tablets supplied by a generic drug supplier.

The RFS methods are flexible, time-efficient and practical in the study of pharmaceutical solids, particularly within a formulated product. Given that selective signal excitation methods are based on differences in relaxation time, which are unique to individual components, these methods can be used in selective signal excitation for mixtures of different compounds, crystalline polymorphs, and mixtures

of crystalline and amorphous forms of the same chemical compounds, as well as in quantitative analysis of these mixtures.

Looking forward, the RFS methods in ^{19}F solid state NMR are expected to enable accurate estimation of the quantitative value in the range of 0.5% to 5% of the target component in the mixture. It is also expected that additional shortening of the experiment duration will further improve the practicality of the methods.

The RFS methods can be applied to not only pharmaceutical sciences, but also in other fields such as wood, soil, food and polymer sciences etc. Further, they would be usable by medical sciences by application to MRI.

REFERENCES

1. Singhal D, Curatolo W, Drug polymorphism and dosage form design: a practical perspective. Advanced Drug Delivery Reviews, 2004. 56(3): 335-347.
2. Morris KR, Griesser UJ, Eckhardt CJ, Stowell JG, Theoretical approaches to physical transformations of active pharmaceutical ingredients during manufacturing processes. Advanced Drug Delivery Reviews, 2001. 48(1): 91-114.
3. Heinz A, Strachan CJ, Atassi F, Gordon KC, Rades T, Characterizing an amorphous system exhibiting trace crystallinity: A case study with saquinavir. Crystal Growth & Design, 2007. 8(1): 119-127.
4. Gustafsson C, Lennholm H, Iversen T, Nyström C, Comparison of solid-state NMR and isothermal microcalorimetry in the assessment of the amorphous component of lactose. International Journal of Pharmaceutics, 1998. 174(1–2): 243-252.
5. Loening NM, Keeler J, Morris GA, One-Dimensional DOSY. Journal of Magnetic Resonance, 2001. 153(1): 103-112.
6. Morris KF, Johnson CS, Diffusion-ordered two-dimensional nuclear magnetic resonance spectroscopy. Journal of the American Chemical Society, 1992. 114(8): 3139-3141.

7. Stejskal EO, Tanner JE, Spin diffusion measurements: Spin echoes in the presence of a time-dependent field gradient. Journal of Chemical Physics, 1965. 42(1): 288-292.

8. Antalek B, Windig W, Generalized rank annihilation method applied to a single multicomponent pulsed gradient spin echo NMR data set. Journal of the American Chemical Society, 1996. 118(42): 10331-10332.

9. Zumbulyadis N, Antalek B, Windig W. Scaringe RP, Lanzafame AM, Blanton T, Helber M, Elucidation of polymorph mixtures using solid-state ^{13}C CP/MAS NMR spectroscopy and direct exponential curve resolution algorithm. Journal of the American Chemical Society, 1999. 121(49): 11554-11557.

10. Gilard V, Trefi S, Balayssac S, Delsuc MA, Gostan T, Malet-Martino M, Martino R, Prigent Y, Taulelle F, DOSY NMR for drug analysis., in NMR Spectroscopy in Pharmaceutical Analysis, Wawer I, Holzgrabe U, Diehl B, Editor. 2008, Elsevier: Amsterdam, NL. 269-289.

11. Nishiyama Y, Frey MH, Mukasa S, Utsumi H, ^{13}C solid-state NMR chromatography by magic angle spinning ^{1}H T_1 relaxation ordered spectroscopy. Journal of Magnetic Resonance, 2010. 202(2): 135-139.

12. Apperley DC, Harris RK, Larsson T, Malmstrom T, Quantitative nuclear magnetic resonance analysis of solid formoterol fumarate and its dihydrate. Journal of Pharmaceutical Sciences, 2003. 92(12): 2487-2494.

13. Lefort R, Gusseme AD, Willart JF, Danede F, Descamps M, Solid state NMR and DSC methods for quantifying the amorphous content in solid dosage forms: an application to ball-milling of trehalose. International of Journal of Pharmaceutics, 2004. 280(1-2): 209-219.

14. Offerdahl TJ, Salsbury JS, Dong Z, Grant D, J.W. G, Schroeder SA, Prakash I, Gorman EM, Barich DH, Munson EJ, Quantitation of crystalline and amorphous forms of anhydrous neotame using ^{13}C CPMAS NMR spectroscopy. Journal of Pharmaceutical Sciences, 2005. 94(12): 2591-2605.

15. Park S, Johnson DK, Ishizawa CI, Parilla PA, Davis MF, Measuring the crystallinity index of cellulose by solid state ^{13}C nuclear magnetic resonance. Cellulose, 2009. 16(4): 641-647.

16. Virtanen T; Maunu, SL, Quantitation of a polymorphic mixture of an active pharmaceutical ingredient with solid state ^{13}C CPMAS NMR spectroscopy. International Journal of Pharmaceutics, 2010. 394(1–2): 18-25.

17. Preston CM, Newman RH, Demonstration of spatial heterogeneity in the organic matter of de-ashed humin samples by solid-state ^{13}C CPMAS NMR. Canadian Journal of Soil Science, 1992. 72(1): 13-19.

18. Zumbulyadis N, Selective carbon excitation and the detection of spatial heterogeneity in cross-polarization magic-angle-spinning NMR. Journal of Magnetic Resonance (1969), 1983. 53(3): 486-494.

19. Frydman L, Olivieri AC, Diaz LE, Frydman B, Morin FG, Mayne CL, Grant DM, Adler AD, High-resolution solid-state ^{13}C NMR spectra of porphine and 5,10,15-20-tetraalkylporphyrins: Implications for the N-H tautomerization process. Journal of the American Chemical Society, 1988. 110(2): 336-342.

20. Saito K, Martineau C, Fink, G, Taulelle F, Flip-back, an old trick to face highly contrasted relaxation times: Application in the characterization of pharmaceutical mixtures by CPMAS NMR. Solid State Nuclear Magnetic Resonance, 2011. 40(Copyright (C) 2012 American Chemical Society (ACS). All Rights Reserved.): 66-71.

21. Tegenfeldt J, Haeberlen U, Cross polarization in solids with flip-back of I-spin magnetization. Journal of Magnetic Resonance (1969), 1979. 36(3): 453-457.

22. Barry SJ, Pham TN, Borman PJ, Edwards AJ, Watson SA, A risk-based statistical investigation of the quantification of polymorphic purity of a pharmaceutical candidate by solid-state ^{19}F NMR Analytica Chemica Acta, 2012. 712(0): 30-36.

23. Brus J, Urbanova M, Sedenkova I, Brusova H, New perspectives of ^{19}F MAS NMR in the characterization of amorphous forms of atorvastatin in dosage formulations. International Journal of Pharmaceutics, 2011. 409(1–2): 62-74.

24. Urbanova M, Brus J, Sedenkova I, Policianova O, Kobera L, Characterization of solid polymer dispersions of active pharmaceutical ingredients by ^{19}F MAS

NMR and factor analysis. Spectrochimica Acta Part A: Molecular and Biomolecular Spectroscopy, 2013. 100(0): 59-66.

25. Ando S, Harris RK, Hazendonk P, Wormald P, Selective NMR pulse sequences for the study of solid hydrogen-containing fluoropolymers. Macromolecular Rapid Communications, 2005. 26(5): 345-356.

26. Montina T, Hazendonk P, Wormald P, Iuga D, The refocused discrimination induced by variable amplitude minipulses (DIVAM) experiment - Improved domain selection in semicrystalline fluoropolymers by ^{19}F solid state nuclear magnetic resonance spectroscopy. Canadian Journal of Chemistry, 2011. 89(9): 1065-1075.

27. Wormald P, Ameduri B, Harris RK, Hazendonk P, Fluorine-19 solid state NMR study of vinylidenefluoride polymers using selective relaxation filters. Solid State Nuclear Magnetic Resonance, 2006. 30(2): 114-123.

28. Wang J, Sánchez-Roselló M, Aceña JL, del Pozo C, Sorochinsky AE, Fustero S, Soloshonok VA, Liu H, Fluorine in pharmaceutical industry: Fluorine-containing drugs introduced to the market in the last decade (2001-2011). Chemical Reviews, 2013. 114(4): 2432-2506.

29. Shete G, Puri V, Kumar L, Bansal A, Solid state characterization of commercial crystalline and amorphous atorvastatin calcium samples. AAPS PharmSciTech, 2010. 11(2): 598-609.

30. Wang WD, Gao X, Strohmeier M, Wang W, Bai S, Dybowski C, Solid-state NMR studies of form I of atorvastatin calcium. The Journal of Physical Chemistry B, 2012. 116(11): 3641-3649.

31. Lubach JW, Munson EJ, Solid-state NMR spectroscopy, in: Hilfiker, R. (Eds). Polymorphism: in the Phrmaceutical Industry; Wiley-VCH, Weinheim, 2006: pp. 81-93.

32. Lubach JW, Xu D, Segmuller BE, Munson EJ, Investigation of the effects of pharmaceutical processing upon solid-state NMR relaxation times and implications to solid-state formulation stability. Journal of Pharmaceutical Sciences, 2007. 96(4): 777-787.

33. Sullivan MJ, Maciel GE, Spin dynamics in the carbon-13 nuclear magnetic resonance spectrometric analysis of coal by cross polarization and magic-angle spinning. Analytical Chemistry, 1982. 54(9): 1615-1623.

34. Fung BM, Khitrin AK, Ermolaev K, An improved broadband decoupling sequence for liquid crystals and solids. Journal of Magnetic Resonance, 2000. 142(1): 97-101.

35. Bennett AE, Rienstra CM, Auger M, Lakshmi KV, Griffin RG, Heteronuclear decoupling in rotating solids. The Journal of Chemical Physics, 1995. 103(16): 6951-6958.

36. Okumura T, Ishida M, Takayama K, Otsuka M, Polymorphic transformation of indomethacin under high pressures. Journal of Pharmaceutical Sciences, 2006. 95(3): p. 689-700.

37. Watanabe A, About the Dimorphism from α-Bromoisovalerylurea (in Germany and Japanese). YAKUGAKU ZASSHI, 1938. 58(6): 565-571.

38. Ohnishi N, Yokoyama T, Kiyohara Y, Kita Y, Kuroda K, Kinetic Study on the Isothermal Transition of Bromovalerylurea Polymorphs in the Solid State at High Temperature. Chemical and Pharmaceutical Bulletin, 1987. 35(3): 1207-1213.

ACKNOWLEDGEMENTS

To write up this thesis, the deepest respect and gratitude for Professor Shigeru Itai of Department of Pharmaceutical Engineering and Drug Delivery Science, School of Pharmaceutical Sciences, University of Shizuoka, for genius support and encouragements to the author.

Special thanks to professors Naoto Oku, Yoshitaka Hamashima and Hiroshi Hashimoto of School of Pharmaceutical Sciences, University of Shizuoka, for their great support and much useful advice.

Gratefully acknowledge to Dr. Takayuki Nemoto of Oral Solid Dosage Analytical Development Dept., Research & Development Division, Teva Pharma Japan Inc., for useful and sympathetic teachings and many advices.

Great thanks to Dr. Hisashi Mimura of Analytical Research Laboratories, Astellas Pharma Inc., for giving a chance for my work and much useful advice.

Great thanks to Dr. Kazuhiro Sako, President of Astellas Ireland Company LTD., for giving a chance for my work and much useful advice.

Great thanks to Dr. Guy Harris, President of Digital Medical Communications Corporation, for his useful advice and English review.

Finally, the author would like to express her thanks to her parents, her sisters and her husband, for their hearty encouragement and supports on her life.

March 2017

Mamiko Asada

PUBLICATIONS

Nasu M, Nemoto T, Mimura H, Sako K, Development of qualitative and quantitative analysis methods in pharmaceutical application with new selective signal excitation methods for ^{13}C solid-state nuclear magnetic resonance using ^{1}H T_{1rho} relaxation time. Journal of Pharmaceutical Sciences, 2013. 102(1): 154-161.

Asada M, Nemoto T, Mimura H, Sako K, Advanced new relaxation filter-selective signal excitation methods for ^{13}C solid-state nuclear magnetic resonance. Analytical Chemistry, 2014. 86(20): 10091-10098.

Nasu-Asada M, Nemoto T, Mimura H, Pharmaceutical applications of relaxation filter-selective signal excitation methods for ^{19}F solid-state nuclear magnetic resonance: Case study with atorvastatin in dosage formulation. Journal of Pharmaceutical Sciences, 2016. 105: 1233-1238.